THE JOURNAL OF PHYSICAL CHEMISTRY B

ARTICLE

pubs.acs.org/JPCB

Permanent Electric Dipole Moments of Carboxyamides in Condensed Media: What Are the Limitations of Theory and Experiment?

Srigokul Upadhyayula,[†,‡,§] Duoduo Bao,[†,‡] Brent Millare,[†,#] Somaia S. Sylvia,[⊥] K. M. Masum Habib,[⊥] Khalid Ashraf,[⊥,▽] Amy Ferreira,[†,◆] Stephen Bishop,[†] Robert Bonderer,[†] Samih Baqai,[†] Xiaoye Jing,[∥] Miroslav Penchev,[⊥] Mihrimah Ozkan,[⊥,*] Cengiz S. Ozkan,[∥,*] Roger K. Lake,[∥,*] and Valentine I. Vullev[†,‡,§,○,*]

[†]Department of Bioengineering, [‡]Center for Bioengineering Research, [§]Department of Biochemistry, [⊥]Department of Electrical Engineering, [∥]Department of Mechanical Engineering, and [○]Department of Chemistry, University of California, Riverside, California 92521, United States

ABSTRACT: Electrostatic properties of proteins are crucial for their functionality. Carboxyamides are small polar groups that, as peptide bonds, are principal structural components of proteins that govern their electrostatic properties. We investigated the medium dependence of the molar polarization and of the permanent dipole moments of amides with different state of alkylation. The experimentally measured and theoretically calculated dipole moments manifested a solvent dependence that increased with the increase in the media polarity. We ascribed the observed enhancement of the amide polarization to the reaction fields in the solvated cavities. Chloroform, for example, caused about a 25% increase in the amide dipole moments determined for vacuum, as the experimental and theoretical results demonstrated. Another chlorinated solvent, 1,1,2,2-tetrachloroethane, however, caused an "abnormal" increase in the experimentally measured amide dipoles, which the theoretical approaches we used could not readily quantify. We showed and discussed alternatives for addressing such discrepancies between theory and experiment.

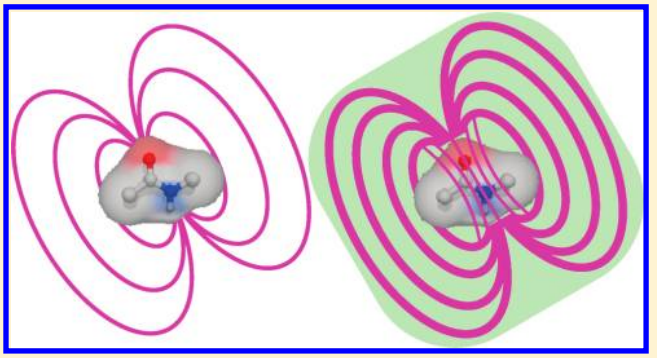

INTRODUCTION

This article describes a comparative study of the ground-state electric dipole moments of six aliphatic carboxyamides (Scheme 1). From experimentally obtained values for the molar polarizations, extrapolated to infinite dilutions, we estimated the permanent electric dipoles of the amides for different solvent media. Concurrently, we determined the amide dipoles theoretically using *ab initio* calculations for vacuum and for condensed media. For chloroform, the independently obtained experimental and theoretical results manifested identical solvent effect on the amide dipoles. For other solvents, however, we observed discrepancy between theory and experiment, which pointed to certain limitations of the used theoretical and experimental approaches.

As vital components of life, proteins have a broad spectrum of functional capacities. Proteins not only provide structural support[1,2] but also drive mechanical movements.[3−5] Proteins mediate active and passive transport,[6−8] as well as signaling,[9−11] and they act as enzymatic entities.[12−15] In addition to the three-dimensional structures, the electrostatic properties of proteins define their reactivity and govern their structure−function relations.[16,17] Local electric fields within the protein environment alter the pK_a values of ionizable functional groups[18] and enable binding selectivity for different types of substrates and for other proteins.[19]

Peptide bonds, which are essentially α-carboxyamides between amino acid residues, are the most essential linkages in proteins. In addition to their role as structural building blocks, peptide bonds contribute significantly to the protein electrostatics. Indeed, amides are small polar groups with permanent electric dipoles exceeding ∼3 D.[20,21]

Scheme 1. Amides with Various Extents of Ethylation

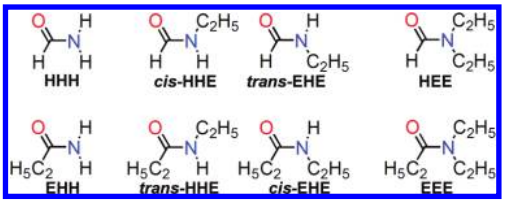

A polypeptide α-helix, for example, supported by a network of hydrogen bonds, is a template for amide bonds with an ordered orientation. The codirectionally oriented amide dipoles, along with the shift in the electron density upon the creation of the hydrogen bonds, generate substantial permanent electric dipole moments for this class of protein conformers; i.e., protein α-helices possess dipole moments amounting to 3−5 D per residue.[22,23] Such electrostatic properties, however, are not

Received: February 20, 2011
Revised: June 16, 2011
Published: June 18, 2011

unique solely for protein α-helices. Protein 3_{10}-helices possess permanent dipole moments of similar magnitude.[24] (3_{10}-helices can be viewed as "tightly wound" α-helices. In fact, α-helices are 3.6_{13}-helices with 3.6 residues per turn and 13-bond loops constrained between every two neighboring hydrogen bonds.[25]) Although polyprolines cannot form intramolecular hydrogen bond, the ordered orientation of peptide bonds in polyproline type I and type II helices also results in considerable permanent electric dipoles that are oppositely oriented for these two types of conformers.[24]

Nature employs such protein electrets for a range of vital functions. (Electrets are materials with ordered electric dipole moments: i.e., they are the electrostatic analogues of magnets.[26,27]) The electric field generated by helix dipoles drives protein binding of charged species,[28] and facilitates the charge-selectivity of ion channels.[29,30] In the vicinity of polypeptide helices, the dipole electric fields rectify the directionality of electron transfer.[24,31,32] Employing oriented amide arrangements in synthetic oligomers allowed for the design of bioinspired electrets.[33,34] Overall, as principal linkers in biological and synthetic polymers,[35−41] the amides and the amide dipoles define the electrostatic properties of macromolecules and govern their functionality.

From readily measurable dielectric quantities, the Debye relation allows for an experimental estimation of the magnitudes of permanent electric dipole moments, $\boldsymbol{\mu}$, of polar molecules:[42]

$$\mu^2 = \frac{9\varepsilon_0 k_B T}{N_A} P_{2\mu}^{(0)} \qquad (1)$$

Here $P_{2\mu}^{(0)}$ is the molar polarization resultant from the field-induced orientation of the molecular dipoles, T is the temperature (in K), and the rest of the quantities are well-known physical constants, i.e., ε_0, the dielectric permittivity of vacuum, k_B, the Boltzmann constant, and N_A, Avogadro's number.

In order to extract intramolecular characteristics from bulk quantities of a solute, the intermolecular interactions in the samples have to be negligible. Hence, gas-phase measurements taken under low-pressure conditions provide the ideal experimental source for estimating molar polarizations for dipole-moment calculations.[43−47] Such experimental requirements, however, present challenges and are implausible for a broad range of molecular species of biological and chemical importance.

As an alternative to gas-phase settings, dielectric and density measurements of binary liquid solutions offer the means for estimating molar polarizations.[48,49] Using nonpolar solvents as major components of such binary solutions provides the means for close to gas-phase microenvironment for the molecular species of interests (which are introduced as the minor components of the binary systems).

To further avoid intermolecular interactions, such as aggregation, the molar polarizations are extracted from diluted solutions. Such dilutions of the analyte, however, decrease the signal-to-noise ratios and places demands on the precisions of the measurements. Extrapolation to infinite dilutions, developed initially by Hedestrand[50] and consequently by Halverstadt and Kumler,[51] provides the means for accessing bulk quantities that reliably characterize intramolecular properties.[52]

The extrapolation of dielectric and density characteristics to zero-solute concentrations yields the total molar polarization, $P_2^{(0)}$. The pronounced difference between the time scales of the various modes of polarization allows for an approximation of the total molar polarization, $P_2^{(0)}$, as an additive quantity of the orientation or dipole, $P_{2\mu}^{(0)}$, vibrational or atomic, $P_{2\nu}^{(0)}$, and electronic, $P_{2e}^{(0)}$, molar polarizations:

$$P_2^{(0)} = P_{2\mu}^{(0)} + P_{2\nu}^{(0)} + P_{2e}^{(0)} \qquad (2)$$

Assuming that $P_{2\mu}^{(0)}$ is the principal component of $P_2^{(0)}$ and that $P_{2\nu}^{(0)}$ and $P_{2e}^{(0)}$ are solely correction terms permits the use of the values of the total polarization as an approximation for the orientation polarization. Implementing such an approximation, i.e., $P_{2\mu}^{(0)} \approx P_2^{(0)}$, for dipole-moment calculations from experimental measurements (eq 1), has proven quite acceptable, especially when the solute dipoles are considerably larger than the solvent dipoles.[48,51] Alternatively, the polarizability of the solute, obtained from its refractivity at off-resonance excitation with visible light, can account for its molar electronic polarization.[48,50] Therefore, high-frequency excitation allows for an estimation of the fast-response electronic polarization, while low-frequency excitation yields the cumulative effect of the total polarization. Decoupling the estimation of the vibrational from the orientation polarization, however, is still an experimental challenge.

Despite a strong preference for nonpolar solvents that do not exhibit specific interactions with the analyte molecules, the use of nonpolar media presents significant experimental drawbacks, such as limited solubility. Furthermore, idealized gas-phase conditions (or condensed-phase conditions that imitate gas phase) are not truly representative of a condensed-phase environment—important, for example, for biological and materials systems.[53] Accounting for media polarization is essential for analyzing the effects of the microenvironment on ions and dipoles in proteins and other biological systems.[53]

While an increase in the solvent polarity may address the above issues, it introduces effects due to electrostatic solute−solvent interactions that can be prevalent even in the absence of specific intermolecular bonding.[54] Polar and/or polarizable solvent molecules, when surrounding a polar solute molecule, react to the electric field from the permanent electric dipole of the solute. As a result, the ordered solvent molecules produce a reaction field in the solvated cavity, enhancing the dipole moment of the solute.[55]

By accounting for the reaction field in a cavity of a solvated polar molecule, Onsager theory has provided an excellent foundation for relating molecular dipoles to bulk dielectric properties of continuous media.[55] As Onsager has pointed out, his theory operates on certain assumptions which undermine its applicability, such as the following: (1) the assumption of spherical molecular shapes; (2) the assumption of incompressibility, i.e., the sum of the molecular volumes equals to the total sample volume; and (3) the assumption of weak short-distance intermolecular interactions, i.e., short-distance interaction energies do not exceed k_BT. Despite these shortcomings, further developments of Onsager theory for nonspherically shaped molecules in nonpolar media,[56,57] hydrogen-bonding environments,[58] and approximations for polar binary solutions[59] have proven promising for the analysis of experimental results.

Herein, we experimentally estimated the electric dipole moments of six amides (Scheme 1) from zero-concentration extrapolations for three solvents with different polarities: 1,4-dioxane (DO), chloroform ($CHCl_3$), and 1,1,2,2-tetrachloroethane (TCE). The solvent effects on the estimated dipole moments correlated with dielectric properties of the media. Using density functional theory (DFT), we also theoretically obtained the dipole moments of the same amides for vacuum and for five solvents: DO, $CHCl_3$, and dimethyl sulfoxide (DMSO), as well

as tetrachloroethene (C_2Cl_4), which has similar polarizability to that of TCE, and dichloromethane (CH_2Cl_2), which has similar static dielectric permittivity to that of TCE. The effects of the condensed media on the *ab initio* calculations were introduced as cavity reaction fields, based on Onsager solvation theory. Similar to the experimental result, the theoretically obtained dipole moments increased with the increase in the media polarity. The values of the vacuum theoretical dipole moments showed some similarity with the experimentally obtained dipoles for DO, which is relatively nonpolar. The theoretically and the experimentally obtained dipole values for chloroform, conversely, were in an excellent agreement, which demonstrates the role of the reaction field in modulating the electronic properties of polar moieties in condensed media. The effect of the most polar solvents on the *ab initio* computed dipoles, however, were not as pronounced as the experimentally obtained dipoles for TCE (i.e., the most polar solvent we used for the experimental aspects of this study). To elucidate this discrepancy, we reviewed the limitations of the experimental and the theoretical approaches used for estimations of permanent molecular dipoles.

RESULTS AND DISCUSSION

Polarization, Polarizability, and Permanent Dipoles. How do measurable bulk dielectric properties depend on the electronic characteristics of the composing molecules? Media polarization, $\mathbf{P}$, under external electric field, $\mathbf{E}$, involves orientation of permanent molecular dipoles, $\boldsymbol{\mu}_i$, and induced displacement of electron density and nuclei as characterized by molecular polarizability, α_i.[60] Therefore, the electric field that each molecule experiences within a solvation cavity in a media with dielectric constant, ε, comprises two principal components: (1) internal field, $\mathbf{E}^{(i)}$, that polarizes the molecule and (2) the directing field, $\mathbf{E}^{(d)}$, that exerts force to turn the molecule and align the molecular dipole.[60] Similarly, the polarization in the presence of external field has two components: (1) induced polarization, $\mathbf{P}_\alpha$, that encompasses the vibrational and electronic polarization, $\mathbf{P}_\alpha = \mathbf{P}_\nu + \mathbf{P}_e$, and (2) orientation polarization, $\mathbf{P}_\mu$.[60] For ideal solutions composed of H different types of molecules, these polarization components are[60]

$$\mathbf{P}_\alpha = 4\pi\varepsilon_0 \sum_{i=1}^{H} N_i \alpha_i \mathbf{E}_i^{(i)} \tag{3a}$$

$$\mathbf{P}_\mu = \sum_{i=1}^{H} N_i \frac{\mu_i^2}{3k_B T} \mathbf{E}_i^{(d)} \tag{3b}$$

The relation between the total polarization and the applied electric field, $\mathbf{P} = \varepsilon_0(\varepsilon - 1)\mathbf{E}$, yields:[60]

$$(\varepsilon - 1)\mathbf{E} = \sum_{i=1}^{H} N_i \left(4\pi\alpha_i \mathbf{E}_i^{(i)} + \frac{\mu_i^2}{3\varepsilon_0 k_B T} \mathbf{E}_i^{(d)} \right) \tag{3c}$$

where N_i is the molecular density (i.e., number of molecules per unit volume) for the ith type of molecules. Considering the reaction field from the solvating media, which allows for relating $\mathbf{E}_i^{(i)}$ with $\mathbf{E}_i^{(d)}$ and with the applied external electric field, $\mathbf{E}$, transforms eq 3c into the various forms of the Onsager equation.[55]

Alternatively, approximating the internal and the directing field to the Lorentz's field, $\mathbf{E}_L$, for an interior of a spherical cavity exposed to external field, $\mathbf{E}$, i.e., $\mathbf{E}_i^{(i)} \approx \mathbf{E}_i^{(d)} \approx \mathbf{E}_L = \mathbf{E}(\varepsilon + 2)/3$, simplifies eq a to the Debye equation:[42,55,60]

$$\frac{\varepsilon - 1}{\varepsilon + 2} = \sum_{i=1}^{H} N_i \left(\frac{4\pi}{3} \alpha_i + \frac{\mu_i^2}{9\varepsilon_0 k_B T} \right) \tag{4a}$$

which for pure liquid transforms into

$$P = N_A \left(\frac{4\pi}{3} \alpha + \frac{\mu^2}{9\varepsilon_0 k_B T} \right) = P_\alpha + P_\mu \tag{4b}$$

The additivity of molar polarization, i.e., $P = \Sigma_i \chi_i P_i$, where χ_i is the mole fraction of the ith component of a mixture, allows for converting the Debye equation into eq 1. For binary isotropic solutions, $H = 2$, therefore, in which the dipole of one of the components is considerably larger than the dipole of the other component, $\mu_2^2 \gg \mu_1^2$ (that is equivalent to $N_2\mu_2^2 \gg N_1\mu_1^2$ for comparable concentrations N_1 and N_2), the predominant term in eq 4a that governs the orientation molar polarization is $\mu_2^2/3\varepsilon_0 k_B T$, permitting one to ignore the term with μ_1 for the less polar compound. Extrapolation to infinite dilutions of the more polar component of such a binary mixture and using $P_{2\mu}^{(0)}$ instead of $P_{2\,\mu}$ allow for approaching idealized conditions, for which the Debye theory is applicable, as depicted in eq 1.

Apparently, at infinite dilution, $\chi_2 \rightarrow 0$, the inequality condition, $N_2\mu_2^2 \gg N_1\mu_1^2$, cannot hold because $\lim_{\chi_2 \to 0} (N_2) = 0$. Conversely, the inequality $N_2\mu_2^2 \gg N_1\mu_1^2$ needs to be valid under the conditions of the experimental measurements of the dielectric properties of the binary mixtures. The extrapolation to zero concentration allows for the following approximations for the dielectric and density properties of the binary solutions: $\lim_{\chi_2 \to 0} (\varepsilon) = \varepsilon_1$, $\lim_{\chi_2 \to 0} (\rho) = \rho_1$, $\lim_{\chi_2 \to 0} (\chi_1) = 1$, and $\lim_{\chi_2 \to 0} (P_2) = P_1^{(0)}$.[50] Therefore, $P_2^{(0)}$ and P_2 are not identical: $P_2^{(0)}$ encompasses the solvent effects of the measurements as this study reveals for the dipole moments of the aliphatic amides.

Another important consideration involves the unfeasibility to carry any of the measurements at close-to-equal concentrations of the two components of the binary mixtures. At $N_1 \approx N_2$ in condensed phase, the interactions between the molecules of the polar component make it prohibitively unfeasible to apply the Debye theory. Therefore, experimental studies are usually conducted at $N_1 \gg N_2$, which allows validity of $N_2\mu_2^2 \gg N_1\mu_1^2$ only if the molecules of the solvent (the predominant component) have no or negligible permanent electric dipole moment, i.e., $\mu_1 \approx 0$. Nevertheless, a number of examples of reliable estimation of the dipole moments of small polar molecules from dilute solutions in solvents with permanent dipoles, such as toluene ($\mu_1 = 0.36$ D), 1,4-dioxane ($\mu_1 = 0.45$ D), and acetone ($\mu_1 = 2.9$ D),[48] illustrate that eq 1 is applicable to cases of $N_1 \gg N_2$ and $\mu_1 > 0$. That is, the extrapolations to zero concentrations, $\chi_2 \rightarrow 0$, from diluted solutions yield $P_2^{(0)}$ values that are representative of the extrapolations from concentrated binary solutions with assumingly idealized no intermolecular interactions between their polar components.

Strictly speaking, polarization represents dipole density, i.e., number of dipoles per unit volume aligned or induced by the applied field. As such a quantity, therefore, $\mathbf{P}$ has the dimensions of charge time distance over volume, or charge over area, as depicted in eqs 3a and 3b. Similarly, polarizability represents the dipole induced in a molecule by the field, and its dimensions should be dipole over field strength, or dipole time distance over potential. As most frequently written in different forms of the Debye equation, the polarizability, α, has dimensions of $\mu^2/k_B T$,

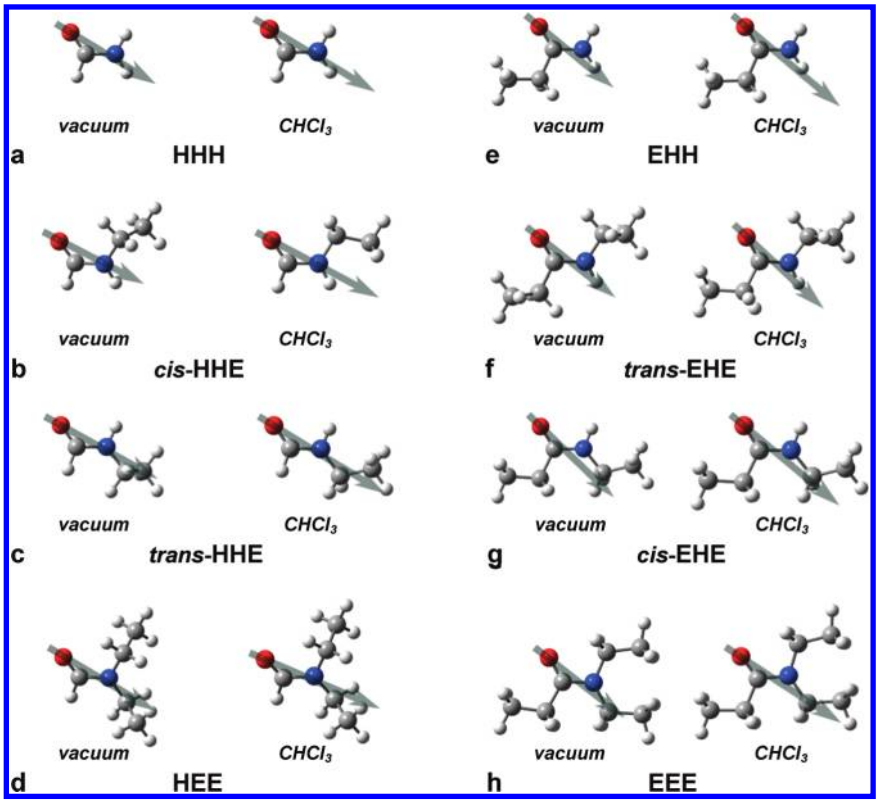

Figure 1. Balls and sticks models of the amide structures, optimized in vacuum and in chloroform ($CHCl_3$). The gray arrows designate the magnitudes and directions of the calculated permanent dipole moments. The direction of the dipole vectors is from their negative to their positive poles.

which, indeed, has the units of dipole time distance over potential. Conventionally, however, polarizability is expressed in units of volume and the molar polarization, P, in units of volume per mole, as depicted in eqs 1 and 4b.

The Lorentz−Lorenz equation (i.e., a Clausius−Mossetti expression involving the dynamic dielectric constants) relates the bulk dielectric properties of a substance with the polarizability of its molecules with radii, r:

$$\alpha_i = \frac{\varepsilon_i(\omega_\alpha) - 1}{\varepsilon_i(\omega_\alpha) + 2} {r_i}^3 = \frac{3}{4\pi} \frac{(\varepsilon_i(\omega_\alpha) - 1)}{(\varepsilon_i(\omega_\alpha) + 2)} v_i \qquad (5a)$$

$$P_{i\alpha}^{(0)} = \frac{(\varepsilon_i(\omega_\alpha) - 1)}{(\varepsilon_i(\omega_\alpha) + 2)} \frac{M_i}{\rho_i} = \frac{4\pi}{3} N_A \alpha_i \qquad (5b)$$

where, for samples composed of molecular species i, v_i is the molecular volume, assuming spherical shape, M_i is the molecular weight, ρ_i is the density, and $\varepsilon_i(\omega_\alpha)$ is the dynamic dielectric constant measured at frequency, ω_α. (eq 5b represents the transformation from 4a to 4b.) The field polarization frequency, ω_α, is high enough so that the molecular permanent dipoles remain stationary (i.e., the molecules cannot turn fast enough to reorient their dipoles along the oscillating electric field), yet ω_α is low enough so that the electron density and nuclei of the molecules can reorganize in phase with the oscillating field. That is, $\varepsilon_i(\omega_\alpha)$ represents the dielectric properties under condition where the orientation polarization is negligible and the total polarization is governed by its vibrational and electronic components.

Experimental determination of $\varepsilon_i(\omega_\alpha)$ at such intermediate frequencies, however, is somewhat challenging. Most frequently, the experimental polarizabilities are estimated from dynamic dielectric properties recorded at optical frequencies where only the electronic polarization is prevalent:

$$\alpha_{ie} = \frac{3}{4\pi} \frac{({n_i}^2 - 1)}{({n_i}^2 + 2)} \frac{M_i}{\rho_i N_A} \qquad (6a)$$

$$P_{ie}^{(0)} = \frac{({n_i}^2 - 1)}{({n_i}^2 + 2)} \frac{M_i}{\rho_i} \qquad (6b)$$

where n_i is the index of refraction of molecular species i, recorded at off-resonance optical frequency, ω_e, i.e., for nonmagnetic compounds, ${n_i}^2 = \varepsilon_i(\omega_e)$.

In general, the electronic polarization is the prevalent component of the induced polarization, i.e., usually $\varepsilon_i(\omega_\alpha) \approx 1.05\varepsilon_i(\omega_e)$. Therefore, eqs 6a and 6b provide a reasonable approximation of eqs 5a and 5b for estimation of the induced polarization and polarizability from experimentally readily measurable quantities.

Theoretical Dipole Moments of Amides. For this study, we selected six aliphatic amides with different extent of alkylation (Scheme 1), i.e., with a hydrogen (Hxx) or an ethyl (Exx) attached to the carbonyl carbon, and with no ethyl (xHH), one ethyl (xHE), or two ethyl substituents (xEE) on the amide nitrogen (where "x" designates "H" or "E"). We calculated the ground-state electric dipole moments of the amides using *ab initio* density functional theory (DFT) as implemented by Gaussian (Figure 1).[61,62]

The implemented computational tools allowed for a separate analysis of the *cis* and *trans* conformers of each of the N-monoethylated amides, HHE and EHE (Figure 1, parts b, c, f, and g). The *cis*-HHE and *trans*-EHE were viewed as analogous because

Table 1. Electric Dipole Moments and Polarizabilities, α, of Aliphatic Amides Determined Theoretically for Vacuum and for Solvent Media with Different Polarities[a]

		μ_2^*/D					α_2^b/Å^3			
amide	$\mu_2^{(0)}$/ D	DO (ε_1 = 2.2)	C_2Cl_4 (ε_1 = 2.5)	$CHCl_3$ (ε_1 = 4.8)	CH_2Cl_2 (ε_1 = 8.9)	DMSO (ε_1 = 47)	α_{xx}	α_{yy}	α_{zz}	$\langle\alpha_2\rangle^c$
HHH	3.74	4.19	4.20	4.49	4.63	4.80	3.08	4.40	5.65	4.38
HHE	3.72[d]	4.41[d]	4.43[d]	4.70[d]	4.80[d]	4.96[d]				8.14[e]
cis	3.69	4.36	4.37	4.69	4.84	5.02	6.16	8.12	10.1	8.13
trans	3.98	4.46	4.47	4.93	4.75[f]	4.87	6.11	7.76	10.7	8.18
HEE	3.78	4.20[f]	4.21[f]	4.49[f]	4.63[f]	4.79[f]	9.80	12.3	13.6	11.9
EHH	3.51	3.97	3.99	4.32	4.47	4.67	6.33	8.23	9.60	8.05
EHE	3.36[g]	3.79[g]	3.85[g]	4.24[g]	4.31[g]	4.49[g]				12.0[e]
trans	3.36	3.78	3.84	4.23	4.27[f]	4.47[f]	9.95	11.0	14.9	12.0
cis	3.76	4.24	4.25	4.58	4.74	4.91	9.13	11.6	15.2	12.0
EEE	3.67	4.16	4.17	4.52	4.69	4.89	11.7	16.0	19.2	15.6

[a] Theoretical values for the magnitudes of the dipole moments from DFT calculations: $\mu_2^{(0)}$, vacuum or gas-phase calculations; μ_2^*, calculations that include the solvent effect using the Onsager formalism. DO = 1,4-dioxane; C_2Cl_4 = tetrachloroethene; $CHCl_3$ = chloroform; CH_2Cl_2 = dichloromethane; and DMSO = dimethyl sulfoxide. [b] The nonzero components of the diagonalized polarizability tensor, α_{ii}, were the eigenvalues of the $\alpha_2 = [\alpha_{ij}]$ matrices obtained from DFT calculations of relaxed structures in vacuum. [c] Average polarizability: $\langle\alpha_2\rangle = (\alpha_{xx} + \alpha_{yy} + \alpha_{xx})/3$. [d] Obtained from weighed sums of the calculated dipoles of the *cis* and *tans* conformers: $(\chi_{cis}\mu_{cis} + \chi_{trans}\mu_{trans})/(\chi_{cis} + \chi_{trans})$; $\chi_{trans}/\chi_{cis} = \exp(-\Delta\mathcal{E}/k_BT)$;$\Delta\mathcal{E} = \mathcal{E}_{trans} - \mathcal{E}_{cis}$; where the DFT-calculated total energies for the HHE conformers are as follows: (1) $\mathcal{E}_{trans} = -6754.39$ eV and $\mathcal{E}_{cis} = -6754.44$ eV for vacuum; (2) $\mathcal{E}_{trans} = -6754.50$ eV and $\mathcal{E}_{cis} = -6754.50$ eV for DO; (3) $\mathcal{E}_{trans} = -6754.51$ eV and $\mathcal{E}_{cis} = -6754.50$ eV for C_2Cl_4; (4) $\mathcal{E}_{trans} = -6754.50$ eV and $\mathcal{E}_{cis} = -6754.57$ eV for $CHCl_3$; (5) $\mathcal{E}_{trans} = -6754.60$ eV and $\mathcal{E}_{cis} = -6754.60$ eV for CH_2Cl_2; and (6) $\mathcal{E}_{trans} = -6754.63$ eV and $\mathcal{E}_{cis} = -6754.64$ eV for DMSO. [e] Obtained from weighed sums of the calculated average polarizabilities of the *cis* and *tans* conformers for vacuum, $(\chi_{cis}\langle\alpha_{cis}\rangle + \chi_{trans}\langle\alpha_{trans}\rangle)/(\chi_{cis} + \chi_{trans})$. [f] These amide structures did not relax in the solvent media. Therefore, we took the relaxed amide structures for vacuum and placed it in the corresponding solvent in order to calculate the dipole moment (single-point calculation). Our comparisons between the results for other amides that were (1) relaxed in the selected solvent and (2) relaxed in vacuum and then subjected to single-point calculation in the same solvent, however, showed that the values of the dipole moment obtained by either of these two methods do not differ significantly. [g] Obtained from weighed sums of the calculated dipoles of the *cis* and *tans* conformers, where the DFT-calculated total energies for the EHE conformers are as follows: (1) $\mathcal{E}_{trans} = -8891.27$ eV and $\mathcal{E}_{cis} = -8891.16$ eV for vacuum; (2) $\mathcal{E}_{trans} = -8891.36$ eV and $\mathcal{E}_{cis} = -8891.26$ eV for DO; (3) $\mathcal{E}_{trans} = -8891.36$ eV and $\mathcal{E}_{cis} = -8891.26$ eV for C_2Cl_4; (4) $\mathcal{E}_{trans} = -8891.42$ eV and $\mathcal{E}_{cis} = -8891.32$ eV for $CHCl_3$; (5) $\mathcal{E}_{trans} = -8891.45$ eV and $\mathcal{E}_{cis} = -8891.39$ eV for CH_2Cl_2; and (6) $\mathcal{E}_{trans} = -8891.48$ eV and $\mathcal{E}_{cis} = -8891.39$ eV for DMSO.

the nitrogen-bonded ethyls and the carbonyl oxygens were on the same side of the axis of the C−N amide bond (Scheme 1). Similarly, the *trans*-HHE and the *cis*-EHE were analogous because their carbonyl oxygens and N-bonded ethyls were on the opposite sides of the axis of the C−N amide bonds (Scheme 1).

The theoretical values of the dipoles for vacuum, $\mu^{(0)}$, of the eight species ranged from about 3.3 to 3.8 D (Table 1). The values of the dipoles for HHH, HEE, and EHH were in a good agreement with the previously reported values for these amides.[63−65] The amide dipoles pointed from the carbonyl oxygens to the nitrogens (Figure 1) (i.e., the direction of electric dipoles is from their negative to their positive poles). Alkylation of the carbonyl carbons yielded an approximate 3−10% decrease in the magnitude of the dipole moments. Conversely, the monoalkylation of the amide nitrogens had the most pronounced effect on the dipole moments. Placing the N-bonded ethyls and the carbonyl oxygens at opposing positions, i.e., *trans*-HHE and *cis*-EHE (Scheme 1), substantially increased the magnitude of the amide dipoles (Table 1). We ascribed these substituent effects to the electron-donating properties of the ethyls. Alkylation of the carbonyl carbons decreased the polarity of the C═O bond. The polarization of the ethyls extended the separation between the centers of the positive and negative charges of the molecules, and hence increased their dipole moments (for *trans*-HHE and *cis*-EHE).

To examine the solvent effect on the dipole moments, we modified the *ab initio* calculations of the eight amide structures to account for condensed media (Figure 1). The polarization effects of the solvents were taken into account by using the self-consistent isodensity polarizable continuum model (SCI-PCM).[66] Each amide solute, represented by a charge distribution, was embedded in a cavity and was surrounded by the solvent, which was a continuous infinite polarizable dielectric. The cavity was defined based on an isosurface of the total electron density.[66,67]

In order to examine the polarization effects of the solvent media, molecules were relaxed in the presence of the solvent as implemented by the SCI-PCM and the dipole moments were calculated again. The SCI-PCM model provides a plausible explanation for the differences between the dipole moments in vacuum, $\mu_2^{(0)}$, and in condensed media, μ_2^*.[66,67] An increase in the solvent polarity enhanced the solvent effect as indicated by the $\mu_2^*/\mu_2^{(0)}$ ratios, which ranged from 1.1 to 1.4 and was the most pronounced for *cis*-HHE (Table 1).

The molecular charge distribution induces a reaction potential in the condensed solvent media, which acts back on the molecular charge distribution changing the molecular dipole moments.[66,67] The effect of the dielectric can be viewed in terms of image charges. The molecular charges induce image charges of the opposite signs in the dielectric. These image charges further polarize the molecular charges, resulting in increased amide dipole moments. An increase in the media polarity and polarizability enhances these image-charge effects, explaining the trends in the solvent effect (Table 1).

Experimental Dipole Moments for Amides in Nonpolar Media. We used the Hedestrand approach for extrapolating the molar polarizations to infinite dilution from concentration-dependent

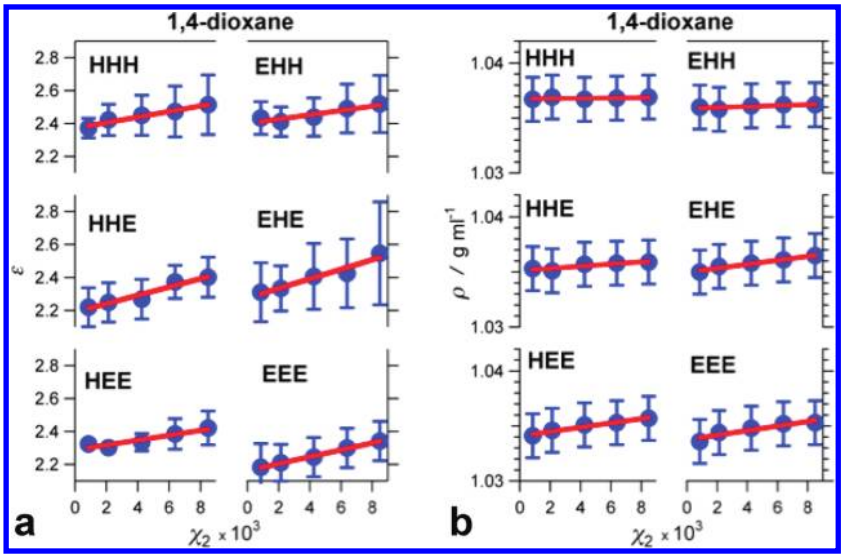

Figure 2. Dielectric and density properties of diluted amide solutions in 1,4-dioxane (DO). Concentration dependence of (a) the solution static dielectric constants, ε, obtained from capacitance measurements, and (b) the solution densities, ρ. The amide concentration is expressed in mole fractions, χ_2. The blue markers represent the experimental data, and the red lines show the linear fits of the data (eq 8).

dielectric and density measurements:[48,50,68]

$$P_2^{(0)} = \frac{3aM_1}{\rho_1(\varepsilon_1+2)^2} + \frac{(\varepsilon_1-1)}{\rho_1(\varepsilon_1+2)}\left(M_2 - \frac{bM_1}{\rho_1}\right) \quad (7)$$

where M_i, ρ_i and ε_i are molecular weights, densities, and static dielectric constants. The subscript "1" designates the quantities for the major component of the binary mixture—the solvent, and "2"—the minor component—the solute, i.e., the amide. The superscript "(0)" designates quantity extrapolated to infinite dilution, i.e., to zero concentration.

While the empirical parameters a and b are extracted from linear fits of the dependence of measured quantities on the moles fraction of the analyte, χ_2 (eq 8a, 8b), they represent the first derivatives of the dielectric constant and of the density, respectively (eq 8c, 8d), of the binary solutions at infinite dilutions (Figure 2):

$$\varepsilon = \varepsilon_1 + a\chi_2 \quad (8a)$$

$$\rho = \rho_1 + b\chi_2 \quad (8b)$$

$$a = \left(\frac{\partial\varepsilon}{\partial\chi_2}\right)_{\chi_2=0} \quad (8c)$$

$$b = \left(\frac{\partial\rho}{\partial\chi_2}\right)_{\chi_2=0} \quad (8d)$$

where the quantities without subscript are for the binary solutions. The coefficients a and b differ from the original Hedestrand coefficients α and β, which were for linear fits normalized to unity intercepts, i.e., $a = \varepsilon_1\alpha$ and $b = \rho_1\beta$.[50] Nevertheless, a facile rearrangement of the original Hedestrand expression yields eq 7, which accommodates the use of a and b instead of α and β.

Ideally, solvents for such studies should be nonpolar, nonhygroscopic, nonvolatile, and nonpolarizable. In addition, solvents with propensities for hydrogen bonding, complexation, and other relatively strong interactions with the solute should be avoided. Therefore, saturated hydrocarbons with high boiling points, and some of their perhaloginated derivatives, present an excellent choice for simulating gas-phase conditions in condensed media.

Our initial studies, employing *n*-hexadecane ($C_{16}H_{34}$) and tetrachloromethane (CCl_4), revealed an important practical issue with the use of such nonpolar solvents. A principal challenge with hydrocarbon solutions proved to be the limited solubility of some of the investigated amides.

For example, from dielectric and density measurements of amide solutions in $C_{16}H_{34}$, the determined dipole moments of HEE and EHE were 3.88 ± 0.15 D and 3.40 ± 0.13 D, respectively, which were in an excellent agreement with the calculated values for vacuum, $\mu_2^{(0)}$, in the absence of solvent effect (Table 1). Conversely, HHH and EHH did not manifest sufficient solubility in $C_{16}H_{34}$ to attain high enough concentrations necessary for measurements with acceptable signal-to-noise ratios. Concurrently, HHE and EEE had acceptable solubility in $C_{16}H_{34}$. The experimentally obtained dipoles for these two amides in $C_{16}H_{34}$, however, were 1.86 ± 0.14 D and 4.59 ± 0.52 D for HHE and EEE, respectively. We ascribed this discrepancy between the experimental dipoles and the corresponding theoretical $\mu_2^{(0)}$ values to the pronounced propensity for aggregation of the amides in nonpolar media. Depending on the size of the aggregates and on the alignment of the amide dipoles in these aggregates, the apparent dipole values, extracted from experimental data, would exceed or be smaller than $\mu_2^{(0)}$.

To address these solubility issues, we explored the use of alternative nonpolar solvents. Because of the symmetry of its molecule, 1,4-dioxane (DO) is one of the least polar ethers with its static and dynamic dielectric constants close in value, i.e., $\varepsilon_1 \approx n_1^2$. In fact, the dielectric constants of DO resembling those of *n*-hexadecane, i.e., for DO, ε_1 = 2.28 and n_1^2 = 2.02; and for *n*-$C_{16}H_{34}$, ε_1 = 2.23 and n_1^2 = 2.05.

From concentration-dependent density and dielectric measurements of amide-DO solutions (Figure 2), we obtained $P_2^{(0)}$ for the six amides (eq 7, 8). Approximating $P_{2\mu}^{(0)}$ to $P_2^{(0)}$ allowed us to use eq 1 to calculate the magnitudes of their dipole moments, μ_2^{**} (Table 2). (While "*" indicates the theoretically calculated

Table 2. Electric Dipole Moments and Molar Polarizations of Aliphatic Amides Determined Experimentally from Dielectric Measurements for Solvent Media with Different Polarities[a]

	$P_2^{(0)b}$/ cm^3 mol^{-1}			μ_2/D					μ_{2C}/ D		
amide	DO	$CHCl_3$	TCE	DO $[p_0/p_{DO}]^e$	$CHCl_3$ $[p_0/p_{CHCl_3}]^e$	TCE	n_2^c	$P_{2e}^{(0)d}$ $[\alpha_{2e}]^f$	DO $[p_0/p_{DO}]^e$	$CHCl_3$ $[p_0/p_{CHCl_3}]^e$	TCE
HHH	255	407	3550	3.51 ± 0.20 [0.10; 0.007]	4.43 ± 0.27 [0.002; 0.55]	13.1 ± 0.7	1.446	11 [4.2]	3.44 ± 0.20 [0.055; 0.005]	4.38 ± 0.27 [—; 0.28]	13.1 ± 0.7
HHE	382	465	[g]	4.29 ± 0.29 [0.03; 0.47]	4.74 ± 0.57 [0.001; 0.84]	[g]	1.430	20 [7.9]	4.18 ± 0.28 [0.047; 0.20]	4.64 ± 0.54 [0.003; 0.76]	[g]
HEE	236	418	1580	3.37 ± 0.32 [0.08; 0.014]	4.50 ± 0.17 [—; 0.87]	8.76 ± 0.11	1.433	29 [12]	3.16 ± 0.30 [0.026; 0.006]	4.34 ± 0.16 [—; 0.036]	8.68 ± 0.11
EHH	271	488	1110	3.62 ± 0.15 [0.24; 0.018]	4.86 ± 0.16 [—; —]	7.34 ± 0.35	1.432[h]	18 [7.2]	3.50 ± 0.15 [0.90; 0.007]	4.77 ± 0.16 [—; —]	7.28 ± 0.35
EHE	442	501	1870	4.62 ± 0.31 [0.004; 0.013]	4.92 ± 0.70 [—; 0.029]	9.52 ± 0.73	1.434	29 [11]	4.47 ± 0.29 [0.005; 0.020]	4.78 ± 0.68 [—; 0.060]	9.45 ± 0.72
EEE	332	454	1810	4.01 ± 0.07 [0.002; 0.023]	4.69 ± 0.18 [—; 0.032]	9.35 ± 0.27	1.440	38 [15]	3.78 ± 0.07 [0.045; 0.001]	4.49 ± 0.17 [—; 0.32]	9.25 ± 0.27

[a] Experimental dipole moments, μ_2^{**}, for the different solvents were calculated using eq 1, in which $P_{2\mu}^{(0)} \approx P_2^{(0)}$. For the corrected experimental dipole moments, μ_{2C}^{**}, we used $P_{2\mu}^{(0)} \approx P_2^{(0)} - P_{2e}^{(0)}$. [b] Molar polarizations were calculated from experimental data for binary solutions of the amides in different solvents using eqs 7 and 8. [c] Amide refractive indexes: measured for the pure compounds that are liquid at room temperature. [d] Molar electronic polarization, in cm^3 mol^{-1}, calculated from experimental n_2 values using eq 6b ($i = 2$). [e] p-values from t-tests of the hypotheses, H_0, that the experimentally determined dipole moments are identical with the theoretically calculated dipoles for vacuum, $p_0 = p(\mu_2^{**} \equiv \mu_2^{(0)})$, for DO, $p_{DO} = p(\mu_2^{**} \equiv \mu_2^{*}(DO))$, and for $CHCl_3$, $p_{CHCl_3} = p(\mu_2^{**} \equiv \mu_2^{*}(CHCl_3))$, where $p(\xi \equiv \zeta)$ is the probability for ξ and ζ to be identical. Dashes, —, in these columns indicate $p < 0.001$. Arbitrarily, for 99% confidence, we reject H_0 when $p < 0.01$. [f] Molecular polarizability, in Å^3, calculated from experimental n_2 values using eq 6a ($i = 2$). [g] Lack of sufficient solubility. [h] EHH is solid at room temperature: we used a published value for its index of refraction, n_2, rather than measuring it as we did for the other five amides.

dipoles for solvent media, "**" designates amide dipoles for different solvents obtained from experimental measurements.)

We further corrected the experimental dipole moments, μ_2^{**}, by the use of a somewhat improved approximation for the orientation polarizations, $P_{2\mu}^{(0)} \approx P_2^{(0)} - P_{2e}^{(0)}$ (eq 2). We estimated the electronic polarization using the dynamic dielectric properties of each amide (eq 6b).[48] The molar electronic polarizations of the six amides, $P_{2e}^{(0)}$, were about 8 to 23 times smaller than the total molar polarizations, $P_2^{(0)}$ (Table 2). Therefore, the values of the corrected experimentally obtained dipole moments, μ_{2C}^{**}, obtained using $P_{2\mu}^{(0)} \approx P_2^{(0)} - P_{2e}^{(0)}$, did not differ significantly from the corresponding dipoles, μ_2^{**}, obtained using $P_{2\mu}^{(0)} \approx P_2^{(0)}$.

To compare the experimentally and theoretically obtained amide dipoles, we employed Student's t-tests. The obtained p-values manifested a lack of trends of identifying similarities between the measured dipoles for DO and the theoretical dipoles for vacuum or for DO (Table 2). Comparison between the experimentally obtained dipoles for DO, μ_{2C}^{**} (Table 2), and the theoretical dipoles for vacuum, $\mu_2^{(0)}$ (Table 1), yielded $p > 0.01$ for all amides except EHE, which prevented us from rejecting the null hypothesis, H_0, (with 99% confidence) about the identity between these experimental and theoretical values (Table 2). Concurrently, comparisons between the measured, μ_{2C}^{**}, and the theoretically calculated, μ_2^{*}, dipoles for DO of the N-monoalkylated amides, HHE and EHE, yielded $p > 0.01$. These results appeared encouraging, indicating that, for these two amides, the DO solvent effect, as implemented by the PCM, correlated well with the experimental findings. We believe, however, that the interpretation of the statistical results did not provide straightforward answers and hence required caution in drawing the conclusions. While $p > 0.01$ did not provide the basis for rejecting H_0, $p < 0.1$ was not necessarily a strong evidence for accepting H_0. Therefore, it was essential to examine closely the experimental and theoretical setups.

Experimentally, the limited solubility in nonpolar solvents justified the need for carrying the analysis with DO. The improved solubility of the six aliphatic amides in this cyclic diether suggested that DO provides solvation interactions that solubilize the polar analytes. Thus, DO is not truly noninteracting solvent, and it would be unacceptable reason to expect identity between the dipole moments measured for DO, μ_2^{**}, and/or μ_{2C}^{**}, and the "true" amide dipoles, $\mu_2^{(0)}$, calculated for vacuum. Therefore, the similarities between the theoretical dipoles in vacuum, $\mu_2^{(0)}$, and the experimental dipoles in DO, μ_{2C}^{**}, were most probably a serendipitous balance between enhancing and reducing solvent effects.

Theoretically, PCM model provides an excellent means for implementation of the Onsager formalism on solvation of molecules with arbitrary shapes. As a continuum model, however, PCM suffers from some deficiencies. The size of the DO solvent molecules is comparable with the sizes of the analyzed amides. Therefore, the arrangement of the DO molecules around the solvation cavity may introduce local effects on the reaction field, for which PCM does not account. DO, indeed, is a nonpolar ether. Its molecule, however, comprises two oxygens that polarize the six-member saturated ring; i.e., the DO molecule contains two oppositely oriented permanent dipoles. The exact effects of these dipoles on the reaction field in the solvation cavity cannot be predicted without vigorous analysis of the arrangement of the DO molecules around the amides.

Furthermore, the PCM model does not account for strong specific interactions, such as intermolecular hydrogen bonding.

While DO is a noninteracting liquid, i.e., the DO molecules do not form hydrogen bonds with one another, DO is a hydrogen-bond acceptor. Four of the amides we studied have amide N−H hydrogens that can readily bond with the free electron pairs on the DO oxygens. Such hydrogen bonding between the DO solvent and the solvated amides causes shifts in the electron density and hence changes in the solute polarization.

Dipole Moments of Amides in Moderately Polar Media. Because of solubility issues, nonpolar media limits the type of polar molecules that are possible to examine. While nonpolar ethers, such as DO, may address the solubility issues, they introduce complexity of local solvation interactions that computationally are not readily implementable. Therefore, we extended our studies to two chlorinated solvents, chloroform ($CHCl_3$) and 1,1,2,2-tetrachloroethane (TCE), which are known for their excellent dissolving properties for organic substances without being hydrogen-bond donors or acceptors.

Although chloroalkane solvents cannot hydrogen bond with solutes, the formation of halogen bonds (X-bonds) with hydrogen-bonded carbonyl oxygens presents a concern.[69] In order for such X-bonding to occur, the solute itself has to form intermolecular hydrogen bonds (which is possible for the four amides that contain nitrogen-bonded hydrogens, i.e., N−H bonds).[69] Avoiding amide aggregation via dilutions ensures avoiding such hydrogen bonding, and hence avoiding X-bonding with the solvent.

The six amides exhibited excellent solubility in $CHCl_3$, and, with the exception of HHE and EHE, the concentration dependence of the dielectric constants was linear for $\chi_2 < 0.01$ (Figure 3a). For the nonlinear trends, we extrapolated the derivatives to zero-concentrations by fitting the data to a power function, i.e., $\varepsilon = \varepsilon_1 + a\,\chi_2 + c\,\chi_2^d$, and hence $(\partial\varepsilon/\partial\chi_2)_{\chi 2=0} = a$ for $d \neq 1$. We, however, limited our analysis to sufficiently diluted solutions (i.e., $\chi_2 < 10^3$) and avoided concentration ranges where the apparent nonlinearity suggested for intermolecular interactions that caused binary solutions to deviate from ideality (Figure 3b).

Using the Debye−Hedestrand relations (eqs 1, 2, 7, and 8), we obtained the values of the dipole moments of the six amides for $CHCl_3$, which were notably larger than the corresponding dipoles for nonpolar media obtained theoretically, $\mu_2^{(0)}$, and experimentally, μ_2^{**} for DO (Table 1 and 2). Introducing the correction for the molar electronic polarization of the amides resulted in a reduction of the dipole values by less than 5% of the uncorrected dipoles (Table 2). Because the values of $P_2^{(0)}$ for chloroform were larger than the corresponding $P_2^{(0)}$ values for 1,4-dioxane, the corrections for $P_{2e}^{(0)}$ were less significant for this more polar media.

The solvent effect on the amide dipoles for TCE media was even more pronounced than the solvent effect we observed for $CHCl_3$. (TCE is a more polar solvent than $CHCl_3$.) With the exception of HHE, the amides were quite soluble in TCE. The dielectric constants of the amide TCE solutions exhibited linear concentration dependence for $\chi_2 < 10^3$ (Figure 3c). The extrapolated $P_2^{(0)}$ values were notably larger than the $P_2^{(0)}$ values we obtained for DO and $CHCl_3$, i.e., 5- to 10-fold larger (Table 2). Therefore, the correction for the molar electronic polarization, $P_{2e}^{(0)}$, had even lesser effect on the experimental dipole values for TCE than for DO or $CHCl_3$, i.e., for TCE, $\mu_{2C}{}^{**} \approx \mu_2{}^{**}$ (Table 2).

For all six amides, the *t*-tests on the identity between the experimental dipoles for chloroform, $\mu_{2C}{}^{**}$, and the theoretical dipoles for vacuum, $\mu_2{}^{(0)}$, yielded *p*-values smaller than 0.01, allowing for an indiscriminate rejection of H_0:$(\mu_{2C}{}^{**} \equiv \mu_2{}^{(0)})$ with 99% confidence for the $CHCl_3$ measurements (Table 2). For TCE, identical *t*-tests yielded $p \ll 0.01$ for the identity between $\mu_{2C}{}^{**}$ and $\mu_2^{(0)}$, which was apparent from the excessively large TCE solvent effect (Table 1 and 2). Indeed, the corrections for molar electronic polarization (eq 6b) did not account for the discrepancies between the experimental dipoles, $\mu_2{}^{**}$, for the chlorinated solvents and the corresponding theoretical values for vacuum, $\mu_2{}^{(0)}$ (Table 1 and 2).

For $CHCl_3$, applying the same statistics for comparing the experimental amide dipoles with the corresponding theoretical dipoles yielded $p > 0.01$ for five of the amides, and $p > 0.10$ for $\mu_2{}^{**}$ or $\mu_{2C}{}^{**}$ of four of these five amides. For EHH, $p < 0.01$. Nevertheless, for EHH, the theoretically calculated value of $\mu_2{}^*$ (for $CHCl_3$) underestimated its experimentally determined dipole moment, $\mu_{2C}{}^{**}$, with only about 10% (Table 1 and 2). These results allowed us to conclude that, within the inherent uncertainty of the used methods, the experimentally obtained amide dipoles for $CHCl_3$, $\mu_2{}^{**}$, or $\mu_{2C}{}^{**}$ are identical with the theoretically calculated dipoles for the same solvent, $\mu_2{}^*$, and different from the theoretically obtained dipoles for vacuum, $\mu_2{}^{(0)}$.

The agreement between theory and experiment for $CHCl_3$, suggested that the reaction field exerted in the solute cavity was the underlying reason for the observed solvent effect on the amide dipoles in chloroform. Furthermore, the results demonstrated that implementation of the solvating media as a continuous dielectric into *ab initio* calculations allowed for quantification of the solvent effect of $CHCl_3$ on the amide dipoles.

The PCM model, however, did not account for the pronouncedly large solvent effects on the amide dipoles experimentally obtained from TCE solutions. We carried SCI-PCM *ab initio* calculations on the six amides, solvated by chlorinated solvents with polarity (i.e., dichloromethane, CH_2Cl_2) and polarizability (i.e., tetrachloroethene, C_2Cl_4) similar to the polarity and polarizability of TCE (Table 3). The theoretically calculated solvent effects, $\mu_2{}^*/\mu_2{}^{(0)}$, for CH_2Cl_2 and C_2Cl_4 ranged between about 10% and 30% (Table 1). The experimentally measured solvent effect, $\mu_2{}^{**}/\mu_2{}^{(0)}$, for TCE, however, ranged between 100% and 250%. This dramatic discrepancy suggested either (1) experimental shortcomings in use of TCE for solvent media (such as analyte aggregation), (2) limitations in the Debye−Hedestrand formalism for analyzing TCE binary mixtures, or (2) limitations in the theoretical treatment of TCE as a dielectric continuum as implemented with the PCM model.

Aggregation. Discrepancies in dipole moment measurements, along with nonlinear concentration dependence of the dielectric constants of binary solutions, are often ascribed to aggregation. We employed ^{1}H NMR spectroscopy to examine the aggregation propensity of the six amides in chloroform and in TCE.[83] (The working concentration range for the dielectric measurements is within the dynamic range of NMR spectroscopy.[84])

For HHH, HEH, EHH, and EHE in $CHCl_3$, the concentration increase from 4×10^{-4} to 8×10^{-3} caused 0.15 to 0.3 ppm downfield shifts in the signals from their amide protons (Figure 4). Ascribing the deshielding (which causes such downfield shifts) to intermolecular hydrogen bonding and to an increase in the dipole-induced polarization of the N−H bonds indicated that aggregation, specifically hydrogen-bonding-assisted aggregation, was plausibly the cause for the observed changes in the chemical shifts of the amide protons.

Although the concentration dependence of the dielectric properties of the HHH and EHH solutions manifested linearity within a relatively broad concentration range, i.e., $\sim 10^{-4} < \chi_2 < \sim 10^{-2}$ (Figure 3a), the concentration-induced changes of the N−H

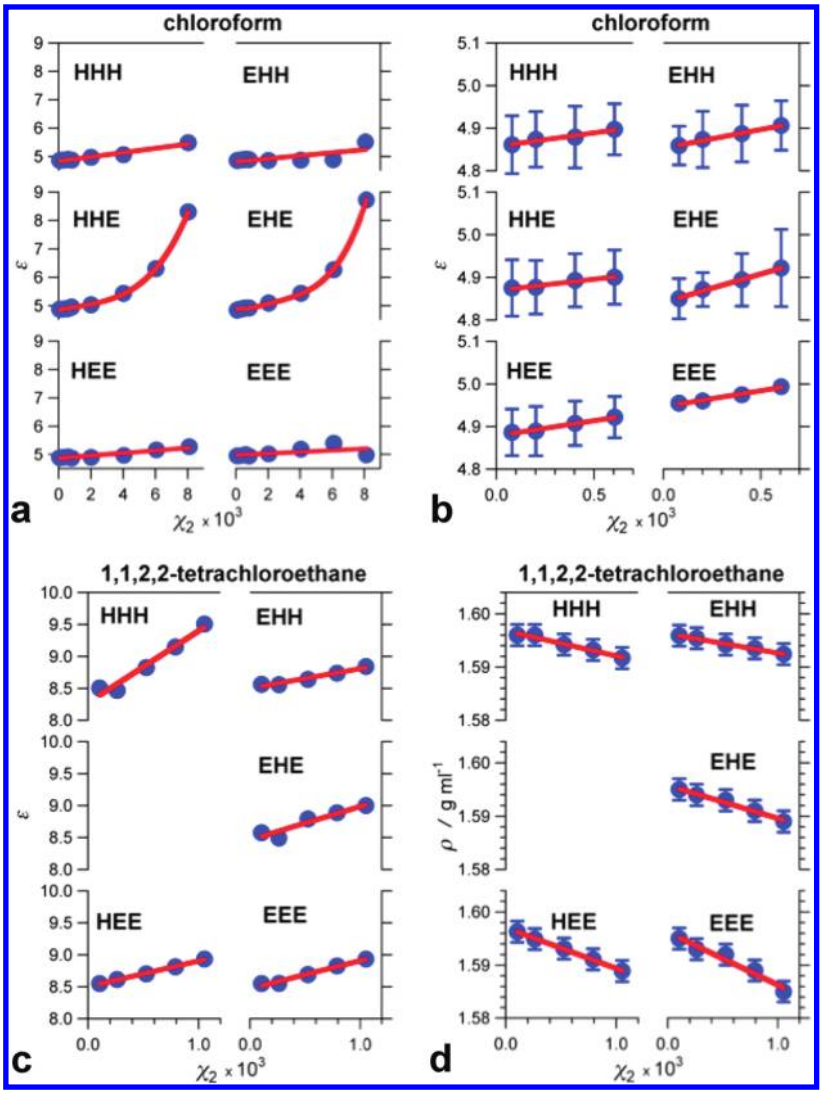

Figure 3. Dielectric and density properties of diluted amide solutions in chlorinated solvents. (a, b, c) Static dielectric constant, ε, obtained from capacitance measurements of amide solutions in (a, b) chloroform ($CHCl_3$), and (c) 1,1,2,2-tetrachloroethane (TCE). (d) Densities of amide solutions in TCE. The concentration of the amides, χ_2, is expressed in mole fractions. The blue markers represent the experimental data, and the red lines represent the data fits.

chemical shifts (Figure 5a,b) were evidence for amide aggregation. These findings were in agreement with the reported propensity of HHH for intermolecular hydrogen bonding.[85−87] Conversely, the observed concentration-dependence of the amide chemical shifts of HHE and EHE (Figure 4c,d), reflected the measured dielectric nonlinearity for $\chi_2 > \sim 2 \times 10^{-3}$ (Figure 3a).

In addition, the N−H chemical shifts of the N-monoalkylated amides, HHE and EHE, revealed an important trend regarding the conformer distribution of these two conjugates. The broad NMR peak of the amide proton of HHE had a shoulder at its downfield side (Figure 4c), consistent with the presence of at least two conformers, i.e., *cis* and *trans* (Scheme 1). Conversely, the amide signal for EHE was a singlet for the investigated concentration range, indicating the detectable presence of only one conformer (Figure 4d). This observation was consistent with the calculated energies of the conformers of these two amides in chloroform (Table 1, footnotes d and g). While the energy difference between the *cis* and *trans* conformers of HHE was 0.03 eV (comparable with k_BT for room temperature), the *cis*−*trans* energy difference for EHE was 0.1 eV. Therefore, the HHE samples contained two principle conformers "locked" by the partial π-conjugation of the C−N bond, and the EHE samples were composed predominantly of the *trans*-amide (Scheme 1): i.e., assuming the Boltzmann distribution for room temperature, more than 98% of EHE existed in its *trans* form.

The concentration-induced changes in the chemical shifts of the methylene, $-CH_2-$, methyl, $-CH_3$, and carbonyl, $-C(=O)-H$, protons were not as extensive as the changes in the signals from the amide protons (Figure 5). The chemical shifts of the carbonyl protons (between 8.0 and 8.3 ppm) remained independent of the amide concentrations (Figure 5a,c,e). Conversely, the protons of the carbonyl-bound methylenes (in the region between 2 and 2.5 ppm), along with the corresponding methyl protons (in the 1−1.3 ppm region), exhibited slight concentration-induced upfield shifts that did not exceed about 0.02 ppm - (Figure 5b,d,f).

The alterations in the shapes of some of the peaks, however, were a conspicuous indication of concentration-induced changes in the molecular microenvironment. For EHH, for example, the concentration increase caused a quadruplet-to-pentaplet

Table 3. Solvent Dielectric Bulk Properties with the Corresponding Molecular Electrostatic Characteristics

	experimental							theoretical[a]					
									α_1^e / Å^3				
solvent	ε_1	n_1^2	γ_1[b]	μ_1** / D	α_{1e}[c]/Å^3	CM*/CM[d]	conformer	$\mu_1^{(0)}$/D	α_{xx}	α_{yy}	α_{zz}	$\langle\alpha_1\rangle$[f]	CM*[g]
DO	2.2	2.011	0.059	0.0−0.45[h]	8.51	0.30/0.29	*chair*	0.00	8.21	8.75	10.1	9.01	0.30
							boat	1.44	8.11	8.47	10.1	8.89	0.81
C_2Cl_4	2.5	2.267	0.041	0.0[i]	12.0	0.30/0.33	—	0.00	7.99	14.5	15.7	12.7	0.39
$CHCl_3$	4.8	2.083	0.27	1.0−1.2[j]	8.43	0.64/0.56	—	1.04	6.72	9.71	9.71	8.71	0.59
TCE	8.4	2.227	0.33	1.3−1.7[k]	12.1	0.86/0.71	*anti*	0.00	9.42	13.7	15.0	12.7	0.36
							gauche	1.58	11.4	12.1	14.3	12.6	0.84
CH_2Cl_2	8.9	2.028	0.38	1.5−1.7[l]	6.46	1.1/0.72	—	1.61	5.23	5.86	8.48	6.53	1.2
DMSO	47	2.187	0.44	3.7−4.4[m]	7.98	6.0/0.94	—	3.82	7.20	8.86	9.15	8.40	4.6

[a] From DFT *ab initio* calculations of relaxed structures in vacuum (Scheme 2). [b] The polarities of the solvents, γ_1, were estimated from their static and dynamic dielectric constants: $\gamma_1 = n_1^{-2} - \varepsilon_1^{-1}$. [c] The experimental solvent polarizabilities, α_{1e}, were calculated from the solvent indexes of refraction, n_1, using eq 6a ($i = 1$). [d] From experimental measurements: CM* from eq 9a for room temperature, using μ_1** and α_{1e}; and CM from eq 9b, using ε_1. [e] The nonzero components of the diagonalized polarizability tensor, α_{ii}, were the eigenvalues of the $\boldsymbol{\alpha}_1 = [\alpha_{ij}]$ matrices obtained from DFT calculations. [f] Average polarizability: $\langle\alpha_1\rangle = (\alpha_{xx} + \alpha_{yy} + \alpha_{xx})/3$. [g] From theoretical calculations: from eq 9a for room temperature, using $\mu_1^{(0)}$ and α_{zz}. [h] References 70−73. [i] Reference 74. [j] References 75−77. [k] References 78 and 79. [l] Reference 80. [m] References 73, 81, and 82.

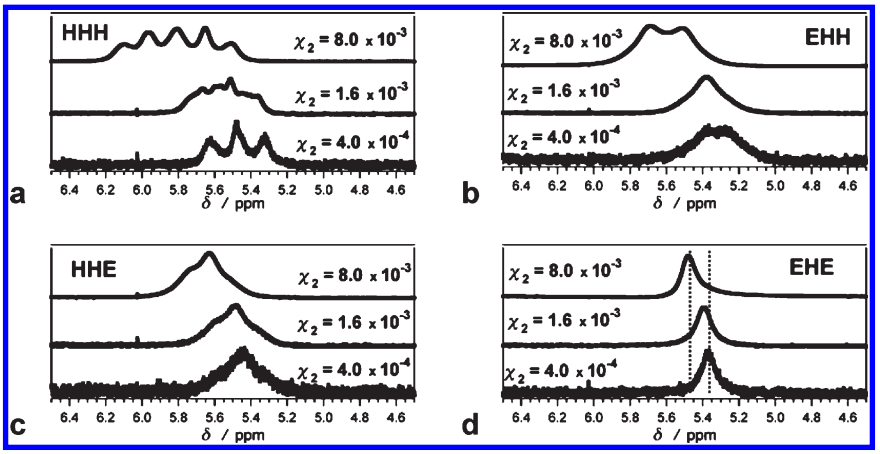

Figure 4. ^{1}H NMR spectra of the amide, N−^{1}H, region, depicting the concentration dependence of the chemical shifts of the N−^{1}H protons for samples dissolved in $CDCl_3$.

conversion of the $-CH_2-$ proton signal and a triplet-to-quadruplet transformation of the $-CH_3$ proton signal (Figure 5b). The changes in peak appearance were not limited to the signals from protons of the carbonyl-bound ethyls. For EEE, for example, upon the concentration increase, the proton signals from the nitrogen-bound methylenes (in the 3−3.5 ppm region), along with the other signals of the other alkyl protons, broadened and manifested an increase in multiplicity (Figure 5e). The significance of the latter observation is that even though EEE cannot undergo intermolecular hydrogen bonding (i.e., EEE is not a hydrogen-bond donor), it still aggregates at elevated concentrations. Therefore, in addition to hydrogen bonding, electrostatic attraction is also a driving force for amide aggregation, even in chlorinated solvents with moderate polarity.

The carbonyl proton of HHE exhibited a strong singlet, at 8.16 ppm, and a weak upfield doublet, at 8.09 ppm (Figure 5c, g), which provided additional information about the distribution of the *cis* and *trans* conformers of this amide. As predominantly governed by the Fermi contact mechanism, the coupling of the carbonyl proton is significantly stronger with the N−H proton located at the *trans* position than with the N−H proton located at the *cis* position.[86] For HHH, for example, the reported through-three-bond coupling constant for the *trans* and *cis* protons are, respectively, $^3J_{trans\text{-}HH} \approx 13$ Hz and $^3J_{cis\text{-}HH} \approx 2$ Hz.[86−88]

For the carbonyl proton doublet of HHE (representing the minor component of the mixture), we determined $J = 12$ Hz (Figure 5g), which allowed us to plausibly ascribe it to the *trans* conformer. The signal from the carbonyl proton of the major component of the HHE mixture, however, appeared as a singlet with a half-height width of ~6 Hz. The peak broadening was the most plausible reason for masking the doublet that resulted from the coupling of the carbonyl proton with the *cis* N−H proton, for which the expected $^3J_{HH}$ would be in the order of 2 Hz.[86] Therefore, we assigned the major component to the *cis*-HHE conformer.

The estimated proton deshielding further supported the above NMR assignments for the HHE *cis* and *trans* conformers. The calculated atomic charges of the carbonyl and methylene protons of the *cis*-HHE were more positive than the charges of the same protons of the *trans* conformer (Figure 5h). Therefore, the downfield shifted signals, representing the major component of HHE (Figure 5c, g), belonged to its *cis* conformer.

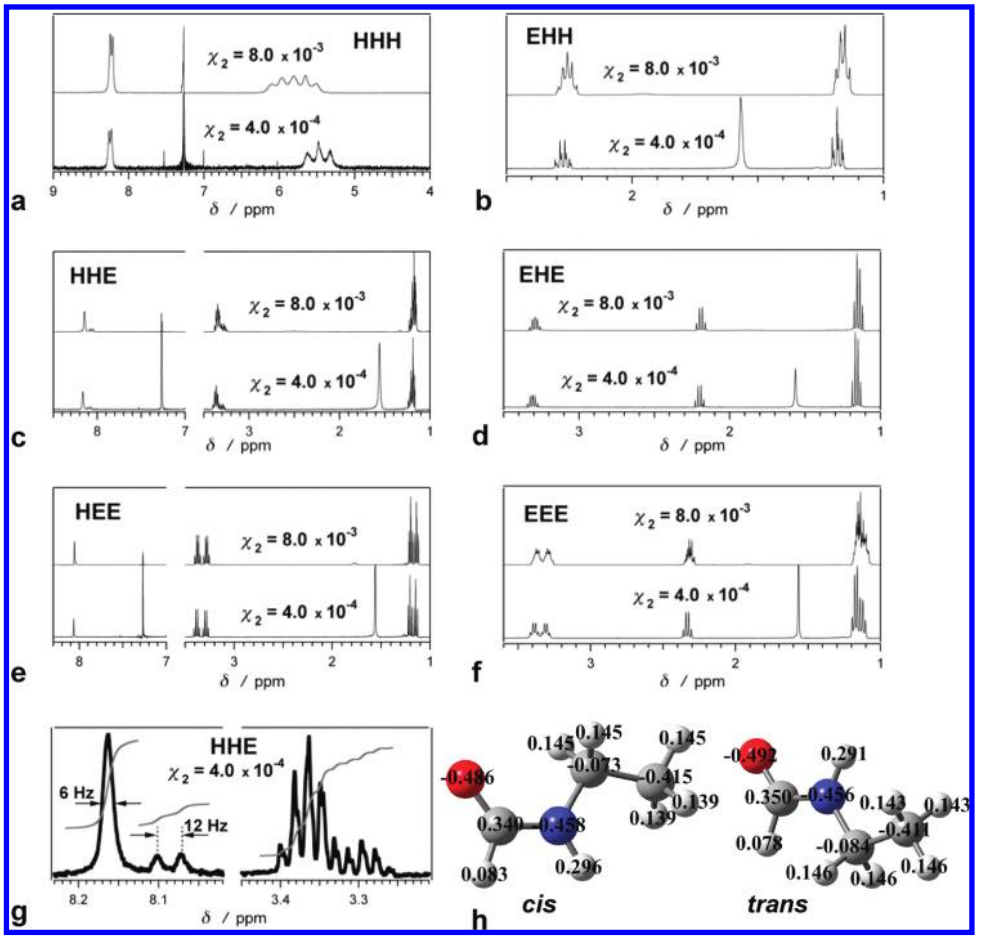

Figure 5. ^{1}H NMR spectra of the carbonyl and aliphatic proton regions of $CDCl_3$ solutions of the six amides. (a, c, e) Chemical shifts of the carbonyl and the aliphatic proton at two different sample concentrations. (b, d, f) Chemical shifts of the aliphatic protons at two different concentrations for the samples with ethylated carbonyls. (g) Chemical shifts of the carbonyl and the methylene protons of HHE showing the presence of two conformers. In part g, the highest peaks in the carbonyl and in the aliphatic region are normalized for clarity. (h) Balls and sticks structures of the two most stable HHE conformers with the corresponding atomic charges calculated for chloroform media. The singlet at 7.27 ppm was from the traces of C^1HCl_3 and was used for internal standard, and the broad singlet at 1.56 ppm was ascribed to traces of water in the solvent.

The areas under the carbonyl and methylene NMR proton peaks, assigned to the two HHE conformers, revealed that at room temperature in chloroform the *cis*/*trans* concentration ratio was: $C_{cis}/C_{trans} = 3.7$ (Figure 6g). Employing the Boltzmann distribution, we estimated the energy difference between the two conformers, i.e., $\Delta E = \mathcal{E}_{trans} - \mathcal{E}_{cis} = 0.033$ eV.

In this analysis, however, we did not take under consideration the energy fluctuations induced by conformational changes in the ethyl groups of the *cis*- and *trans*-HHE structures. The NMR measurements represent the ensemble average from all thermally accessible ethyl conformations that are separated by relatively small energy barriers allowing fast exchange between them within the millisecond duration of signal recording. Conversely, the theoretical values reflected solely the energy differences between the relaxed *cis*- and *trans*-HHE structures (Figure 1).

Nevertheless, these findings regarding the *cis*−*trans* distributions of HHE and EHE, which were independently delivered by our theoretical and experimental analyses, have an important implication for viewing the factors that govern the conformations of amides, and especially, the conformations of peptide bonds in proteins and polypeptides. While the intramolecular steric hindrance may provide intuitive guidelines about the relative stability of *cis* versus *trans* amides, the steric hindrance is not the sole driving force in determining the preference of one conformer over another. In the preferred, *trans*, conformer of EHE, the bulkiest groups, i.e., the two ethyls, are on the opposite sides of the C−N bond (Scheme 1; Table 1, footnote g), which is, indeed, intuitively expected. For HHE, however, the preferred conformer is *cis*, in which the two large substituents, i.e., the ethyl and the carbonyl oxygen, are on the same side of the C−N bond (Scheme 1). Indeed, the carbonyl oxygen is not as large as an ethyl, and hence the steric hindrance in *cis*-HHE is not as pronounced as it is in *cis*-EHE. Nevertheless, for a range of torsion angles, the ethyl and the oxygen of *cis*-HHE have a considerable van der Waals overlap. Therefore, other factors, such as the amide electronic structure, govern the preference of the seemingly less favorable *cis*-HHE over the *trans*-HHE.

NMR studies of the amides, employing deuterated 1,1,2,2-tetrachloroethane (TCE-d_2), revealed trends similar to the trends we observed for $CDCl_3$ (Figure 6). For $\chi_2 > 0.001$, which was above the working concentration range for the dielectric studies (Figure 3c,d), we observed 0.1−0.13 ppm downfield shifts of the signals from the amide, N−H, protons (Figure 6a,b,c). Peak broadening accompanied these shifts. The broadening of the amide

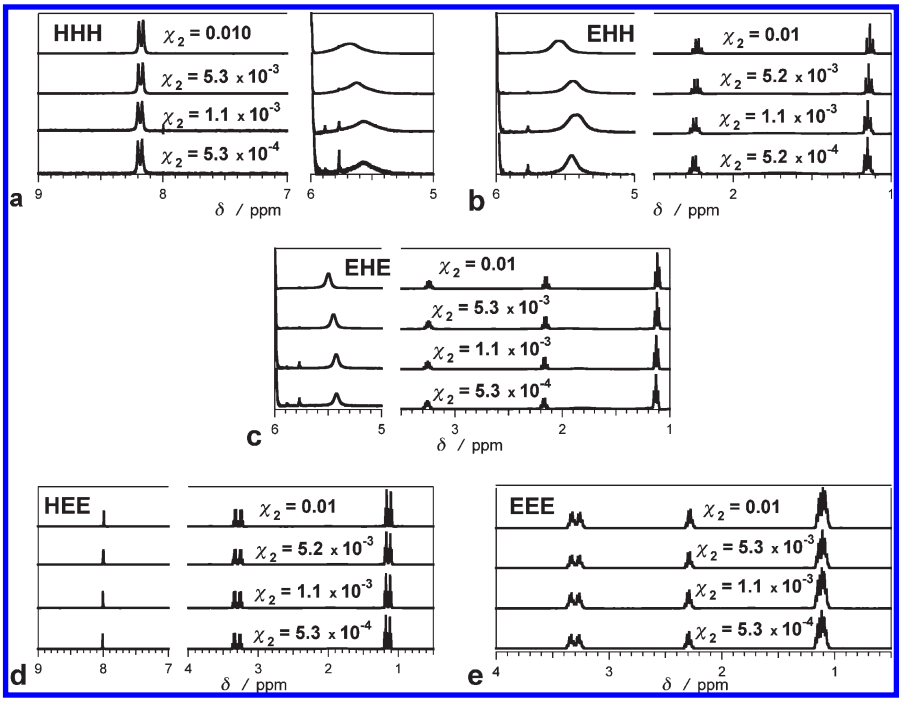

Figure 6. ^{1}H NMR spectra of TCE-d_2 solutions of five of the six amides depicting the concentration dependence (or the lack of concentration dependence) of the chemical shifts of (a, d) the carbonyl protons of Hxx in the 8−8.5 ppm region, (a, b, c) the amide protons of xHx in the 5−6 ppm region, (b−e) the methylene protons of Exx and xxE in the 2−3.5 ppm region, and (b−e) the methyl protons of Exx and xxE in the 1−1.5 ppm region. HHE does not have sufficient solubility in TCE. The solvent peak of TCE-d_1 is at 6 ppm.

peaks revealed a conspicuous distinction between the NMR spectra for $CDCl_3$ and TCE-d_2 solvents. For HHH, for example, the spectra recorded for $CDCl_3$ samples showed a distinct triplet or a multiplet for the amide protons in the 5−6 ppm region (Figure 4a). Conversely, the spectra for TCE-d_2 showed solely a broad singlet for the same amide protons (Figure 6a), an indication for a relatively fast exchange mediated in this solvent.

Overall, the concentration-dependent NMR spectra suggested for amide aggregation at χ_2 exceeding about 0.001. HEE was the only one of the six amides for which we did not observe evidence for aggregation in either of the two chlorinated solvents; i.e., we did not detect concentration-induced changes in NMR shifts of its protons. Thus, the NMR findings validated our choice for conducting the dielectric linear analysis at $\chi_2 < 0.001$ (Figure 3b,c).

Solvent properties. The solvent effects on the ground-state amide electric dipoles reflect the enhancements from the reaction fields in the solvated cavities. As expected, an increase in the static, ε_1, and dynamic, n_1^2, dielectric constant of the solvent media (Table 3), caused an increase in the magnitude of the amide dipoles (Table 1, 2).

The excellent agreement between the experimental and theoretical dipole values for $CHCl_3$, indeed, reflects the plausibility of using continuous-medium models, with the corresponding n_1^2 and ε_1, for *ab initio* analysis of electrostatic properties of polar moieties. The solvent bulk properties, however, did not intuitively reflect the experimentally observed pronouncedly large dipole enhancement induced by TCE. While doubling ε_1 (from DO to $CHCl_3$) increased the amide dipoles with about 20−25%, an additional doubling of ε_1 (from $CHCl_3$ to TCE) caused a dipole increase that amounted to three-to-4-fold (Table 2 and 4). Similarly, the TCE-induced dipole enhancement did not follow the linear increments with the increase in n_1^2 between the three solvents (Table 3).

Limitations in the Debye−Hedestrand procedures for extracting dipole moments from experimentally obtained bulk dielectric data may prove to be a plausible reason for the "abnormally" large amide dipoles measured for TCE media. A principal constrain of this formalism is its sole applicability to diluted polar analytes in nonpolar solvents. Limited solubility of many polar solutes in nonpolar solvents, however, presents important experimental limitations. Hence, how polar can the nonpolar solvents be?

A principal reason for the validity of the Debye theory solely for nonpolar solvents is its limitation imposed by the Clausius−Mossetti expression with static dielectric constants, CM, which cannot have values larger than unity (eq 4a).[89] According to the Debye theory, therefore, a nonpolar solvent should have polarity and polarizability that will yield CM < 1:[89]

$$\mathrm{CM}^* = \frac{\rho_1 N_A}{M_1}\left(\frac{4\pi}{3}\alpha_1 + \frac{{\mu_1}^2}{9\varepsilon_0 k_B T}\right) < 1 \qquad (9a)$$

where,

$$\mathrm{CM}^* \approx \mathrm{CM} = \frac{\varepsilon - 1}{\varepsilon + 2} \qquad (9b)$$

According to this expression, the Curie temperature at which CM* = CM = 1 (i.e., $\varepsilon = \infty$) is unrealistically high for polar materials, implying that they are ferroelectric at room temperature. Furthermore, for such polar materials, the equality between CM and CM* as expected from their known dipoles and polarizabilities, CM* ≈ CM (eq 9b), fails, making the Debye formalism inapplicable for them. For DO, $CHCl_3$, and TCE at room temperature, CM* < 1, and within about 20%, CM ≈ CM* (Table 3). Conversely, CH_2Cl_2 and DMSO exhibited CM* > 1, suggesting their inapplicability for studies that require Debye−Hedestrand analysis. (DMSO, furthermore, is a hydrogen-bond

dx.doi.org/10.1021/jp2045383 |J. Phys. Chem. B 2011, 115, 9473–9490

Table 4. Electric Dipole Moments of Aliphatic Amides, Determined Experimentally from Solutions in Chlorinated Solvents Using Ellipsoidal Approximation of the Solvation Cavity (Equation 10)

		$\mu_2^{(0)**}$ / D	
amide	r_1:r_2:r_3	$CHCl_3$	TCE
HHH	3:1:1	1.5	5.5
HEE	2:3:1	2.1	4.5
EHH	4:2:1	2.2	3.9
EHE	2:2:1	3.0	5.4
EEE	2:3:1	2.4	5.3

acceptor.) This criterion readily rejected the use of DMSO and CH_2Cl_2 in such a line of experimental studies. TCE, however, appeared to be a borderline choice. Although for neat TCE, CM* does not exceed unity, its values for some of the conformers were larger than ~0.8 (Table 3). Therefore, an inclusion of the contribution of a polar solute (with $\mu_2 > 4$ D) in eq 9a causes CM* to exceed unity for $\chi_2 > 0.05$, which is more than an order of magnitude larger than the concentration range we used in this study (Figure 3c,d).

The polarities, γ_1, of $CHCl_3$ and TCE are quite similar (Table 3). Furthermore, the magnitudes of the dielectric constants of the six amides exceed several fold the dielectric constants of any of the used solvents. Therefore, the bulk dielectric properties of the solvents do not appear to be a truly discerning criterion between the chloroform-induced and TCE-induced enhancements observed for the amide dipoles.

In addition to the CM criterion (eq 9), considering the molecular electrostatic (e.g., μ_1), electrodynamic (e.g., α_1), and structural properties of the solvents offers a means for elucidating the "abnormal" TCE effect on the measured amide dipoles. Equation 1 was derived from the Debye equation on the assumption that the solvent dipole term, $\mu_1^2/3\varepsilon_0 k_B T$, can be neglected (eq 4a): i.e., $(\mu_1^{(0)})^2 \ll (\mu_2^{(0)})^2$ or $(\mu_1^{(0)}/\mu_2^{(0)})^2 \ll 1$. For the six aliphatic amides, $(\mu_2^{(0)})^2$ ranged from about 12 to 16 D^2 (Table 1). Concurrently, $(\mu_1^{(0)})^2$ of $CHCl_3$ was about 1.1 D^2, and $(\mu_1^{(0)})^2$ of TCE ranged between about 0 and 2.5 D^2, depending on the molecular conformation (Table 1). Therefore, the square dipole ratios, $(\mu_1^{(0)}/\mu_2^{(0)})^2$, for the amides ranged between 0.07 and 0.09 for chloroform and between 0 and 0.21 for TCE. (Herein, we did not discuss the approximation of the Langevin function, $L(y) \approx y/3$ for $y^{-1} \ll 1$, leading to the Debye equation, because of the relatively small field strengths we used for the dielectric measurements, ensuring $\boldsymbol{\mu}\mathbf{E}^{(d)}/k_B T \ll 1$.[89])

It should be noted that due to conformational flexibility, DO and TCE media comprise mixtures of molecular conformers (Scheme 2).[90,91] The calculated dipole moments of DO and TCE showed a pronounced dependence on their molecular conformations (Table 3). Overall, while the dipole of TCE was able to assume values close to 1.6 D, the dipoles of DO and $CHCl_3$ could not considerably exceed about 1.4 D. Therefore, TCE had the capability to generate slightly stronger reaction fields than either DO and $CHCl_3$. The polar conformers of DO and TCE, e.g., *boat* and *gauche* (Scheme 2), however, are not energetically the most favorable. Therefore, the permanent solvent dipoles were not able account by themselves for the pronounced TCE effect.

The polarizabilities of DO and TCE, on the other hand, had a marginal dependence on their molecular conformations (Table 3).

Scheme 2. Solvent Molecular Structures

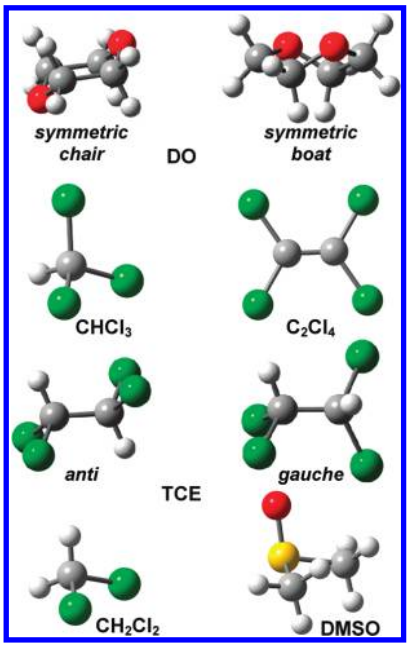

Therefore, generating relatively large induced dipoles in the solvent molecules (needed for noticeable reaction fields in the solute cavities) did not require energetically unfavorable conformations. Furthermore, the wide distribution of the values of the elements of the $[\alpha_{ij}]$ tensor indicated a strong dependence of the solvent polarizabilities on their molecular orientation.

The polarizabilities of $CHCl_3$ and DO were quite comparable. The polarizability of TCE, conversely, exceeded the polarizabilities of $CHCl_3$ and DO (Table 3). These trends in the experimental, α_{1e}, and theoretical, α_{ii} and $\langle\alpha\rangle$, values of the polarizability of the three solvents provided a plausible explanation for the relatively large TCE effect on the amide dipoles.

What Are the Limitations of Theory and Experiment? For experimental estimation of dipole moments of polar moieties in liquid media, it is essential to select noninteracting nonpolar solvents. Conversely, for dissolving a solute even in a nonpolar solvent, that solvent has to be interacting in order to provide sufficient solvation stabilization and prevent aggregation and/or phase separation. Strictly speaking then, all solvents are interacting to some extent. Therefore, for each particular study, the selected solvents ought to be interacting enough to provide sufficient solubility and prevent aggregation and, at the same time, noninteracting enough so that the media polarization around the solvated cavities does not perturb significantly the electronic properties of the analytes.

Assuming that chloroform is one of the most polar solvents applicable for the experimental estimation of the permanent dipoles of aliphatic amides (using the Debye−Hedestrand formalism), revealed the following potential requirement: (1) CM < 1 (eq 9); (2) $(\mu_1^{(0)}/\mu_2^{(0)})^2 < 0.1$; and (3) $\alpha_{1ii} < 10$ Å^3 for solvent molecular volume, v_1, larger than 50 or 100 Å^3. Even when these requirements were met, however, the Debye−Hedestrand analysis of the experimental data produced dipole values that encompassed the enhancement from the reaction field of the solvation cavity (Table 2).

Experiments do not provide means for measuring dipole moments directly. It is the Debye−Hedestrand formalism that

dx.doi.org/10.1021/jp2045383 |J. Phys. Chem. B 2011, 115, 9473–9490

allowed us to extract the values of the dipole moments from dielectric and density measurements (eqs 1, 2, 7, and 8). Like many theories and formalisms developed in the beginning of the 20th century or earlier, the Debye theory approximates the "real systems" to idealized solutions, composed of spherical solute molecules, and nonpolar solvents that pack closely around the solute spheres. Because of its simplicity, however, the Debye theory has been widely used and preferred for relating experimentally obtained bulk dielectric characteristics of materials to the molecular electronic properties of the comprising molecules. Indeed, Debye−Hedestrand analysis of experimental data of relatively simple molecules has produced results in an excellent agreement with theoretical *ab initio* predictions.[48,49] Spherical approximation of the solvated cavities, have yielded theoretical results for complex molecules that agreed well with the experimental findings.[92] Such spherical approximations for molecules with heterogeneous distribution of electron density, however, result in significant discrepancies.[62] Adopting nonspherical representations (with increased complexity) that are representative of the molecular shapes, has the ability to provide a means for agreement between theory and experiment.[62,93]

For the analysis of the amide experimental dielectric data, we tested a model for solvated molecules with ellipsoidal shapes, which is an approximation for nonpolar media, based on the Onsager theory and the Böttcher formalism[56]

$$(\mu_2^{(0)})^2 = \frac{M_2\varepsilon_0 k_B T}{4\pi\rho_2 N_A}\frac{(\varepsilon_1+(n_2^2-\varepsilon_1)A_1)^2(2\varepsilon_1+1)}{(1+(n_2^2-1)A_1)^2(\varepsilon_1+(1-\varepsilon_1)A_1)\varepsilon_1^2}\left(\left(\frac{\partial\varepsilon}{\partial\chi_2}\right)_{\chi_2=0}+\frac{3\varepsilon_1(\varepsilon_1-n_2^2)}{2\varepsilon_1+n_2^2}\right) \quad (10)$$

where A_1 represents the distortion of the spherical shape of the solvated cavity: i.e., A_1 depends on the ratios between the ellipsoid semiaxes, r_1:r_2:r_3, where the permanent dipole is oriented along r_1.[56]

For the five amides, soluble in TCE, this ellipsoid model yielded dipoles that ranged 3.9 and 5.5 D (Table 4), which were closer to the theoretical values of $\mu_2^{(0)}$ (Table 1) than the dipoles extracted using the Debye−Hedestrand analysis (Table 2). The same ellipsoid model applied to the $CHCl_3$ data, however, underestimated the amide dipoles (Table 4). A principal shortcoming of the Onsager theory, on which the ellipsoid model was based (eq 10), encompasses the assumption of incompressibility.[55] We estimated the volumes of the solvated cavity from density of the pure amides, ρ_2. Because of differences in solvation, the volumes of the solvated amide cavities should vary in different media. Furthermore, the molecules of $CHCl_3$ and TCE have different sizes and shapes (Scheme 2). Hence, most likely the solvated cavities differ in size and shape for the two solvents. Nevertheless, the results from the ellipsoid analysis revealed that deviating from the widely used spherical approximation for the solute shapes has the potential to encompass the experimentally observed solvent effects on the amide dipoles.

On the theoretical side of this study, PCM encompasses the arbitrary shapes of the solute molecules.[94] PCM, however, adopts a spherical approximation of the shapes of the solvent molecules needed for estimation of solvent accessibility.[94] Furthermore, should the solvent and solute molecules have comparable dimensions, the continuum dielectric approximation for the cavity solvation may fail. Therefore, interpretation of the results from calculations for DO, C_2Cl_4, and DMSO media (Table 1), ought to be approached with caution.

Improved multiscale models, such as the QM/MM/continuum computational formalism, indeed, offer the potential to address some of the above issues and to provide insight about the structural and electronic properties of solvated cavities.[95,96] The relative complexity and the computational demand of such multiscale models, however, still prevents their wide implementation as a routine formalism for analysis of experimental findings. In fact, PCM is a multi- or biscale, QM/continuum model,[94] and its successful implementation and agreement with the experimental findings for amides solvated by chloroform is quite encouraging (Table 1 and 2).

CONCLUSIONS

How does one quantify the solvent effects on the dipoles of polar species in condensed media? The simplest and well-tested models frequently impose approximations that are unfeasible for the systems to which they are applied. Conversely, by eliminating the approximations, an increase in the complexity of the models has the potential for bringing agreement between experiment and theory. The rational of such an agreement of theoretical models with experiment, however, does not guaranty that the models describe the underlying phenomena that govern the experimental results. For example, the use of ellipsoid approximation (eq 10) was arbitrary, and it demonstrated trends of improvement in the analysis of the TCE experimental results. It does not claim, however, that the aliphatic amides should fit into ellipsoid solvation cavities. Therefore, an experimental design that produces theoretically testable results with least approximations and assumptions provides the optimal venues toward understanding the investigated phenomena. In this study, the dielectric measurements and the *ab initio* calculations for the amides in chloroform-condensed media, demonstrated an optimal agreement between experiment and theory. Indeed, the many assumptions in the used analysis and formalism did not compromise this agreement.

EXPERIMENTAL SECTION

Materials. The six amides were purchased from TCI America. High purity chloroform, 1,4-dioxane and 1,1,2,2-tetrachloroethane were purchased from Fischer Scientific and Sigma-Aldrich. Caution! 1,1,2,2-Tetrachloroethane is a proven carcinogen (consult with its MSDS). Avoid skin contact and/or inhalation of its vapors.

The binary amide solutions were freshly prepared prior to each measurement and kept at room temperature. We employed amide concentrations that ranged from 1 mM to 100 mM. Using the measured densities of the amide solutions, ρ (e.g., in g L^{-1}), we converted their molarity concentrations, C_2, into mole fraction concentrations, χ_2:

$$\chi_2 = \frac{C_2}{C_1 + C_2} \quad (11a)$$

$$C_1 = \frac{\rho - M_2 C_2}{M_1} \quad (11b)$$

Here M_1 and M_2 are the molecular weights of the solvent and the solute, respectively, and C_1 is the molarity concentration of the solvent.

Dielectric Measurements. For the dielectric measurements, we used: (1) AH2700A ultraprecision capacitance bridge

(Andeen-Hagerling, Inc., Cleveland, OH); and an ultrahigh precision Wheatstone bridge, incorporated into HP 4284A LCR precision meter. Both instruments were connected to a three-terminal capacitance sample cell,[68,97] and the corrections for the connecting cables with up to of 4-m length were enabled.

The cell was filled with about 2 mL sample solution, the electrode separation was set at 400 μm, and the capacitance measurements were carried at frequencies ranging from 10^3 Hz to 10^6 Hz. (Because of the relatively large dissipation factor for the TCE samples, they were measured at frequencies that did not exceed 10^4 Hz) In addition to the amide binary solutions, for controls, we measured the capacitance of the neat solvents and of air (i.e., of an empty dry cell).[98] The dielectric constants of the binary amide solutions were calculated from the parallel capacitance values, corrected for dissipation.[48]

The experimentally determined dielectric values presented in the tables and figures correspond to averages of at least five repeats, where the error bars represent plus/minus one standard deviation. Except for EEE in $CHCl_3$, the multiple repeats were recorded by two or more operators at different times of year, and the samples were using solvents from different bottles. (The relatively small error bars for EEE in $CHCl_3$ reflected the fact that all repeats were carried on samples prepared by the same person from the same solvent source.)

Density Measurements. The densities of the amide solutions were measured with a calibrated Mettler Toledo portable density meter (Densito 30PX). Each measurement (recorded collected at 21 °C ± 0.5 °C) required about 1 mL freshly prepared sample solution. Immediately prior to each measurement, the densitometer was washed several times with the corresponding sample solution. After each measurement, the densitometer was washed with the corresponding neat solvent and nitrogen dried.

NMR Spectroscopy. Proton nuclear magnetic resonance (^{1}H NMR) spectra were recorded on a Varian Inova 400 MHz spectrometer (Varian Inova 400, CA). Chemical shifts for protons are reported in parts per million and are referenced to residual protium in the deuterated NMR solvents, $CDCl_3$ and $DCl_2C-CDCl_2$ (Cambridge Isotope Laboratories, MA) as an internal indicator ($CHCl_3$: δ = 7.27 ppm; and $DCl_2C-CHCl_2$: δ = 6.00 ppm).

To examine the aggregation propensity of the amides in chloroform and in 1,1,2,2-tetrachloroethane, ^{1}H NMR spectroscopy of five concentrations of amides, 5 mM, 10 mM, 20 mM, 50 mM, and 100 mM were recorded (for conversion to mole fractions, we used eq 11). For the analysis, the NMR data were imported in Igor Pro, version 6 (WaveMetrics, Inc.) on MacOS and WindowsXP workstations.[99−104]

Computational Information. We calculated the ground-state electric dipole moments and polarizabilities of the six amides and of the three solvents using *ab initio* DFT as implemented by Gaussian 03 and Gaussian 09.[61] Geometry optimizations were performed at the DFT level using the Restricted PBE[105] exchange correlation functional and the 6-31G(d, p)[106,107] basis set with a relaxation criterion of 4.5×10^{-4} eV Å^{-1}.

The polarization effects of $CHCl_3$ were taken into account by using the self-consistent isodensity polarizable continuum model (SCI-PCM) as implemented by Gaussian.[66] In this model, the solvent was a continuous unstructured infinite polarizable dielectric with a given dielectric constant. Each amide solute, represented by a charge distribution, was embedded in a cavity, and was surrounded by the solvent. The cavity was defined based on an isosurface of the total electron density.[66,67]

The polarizabilities were calculated in Gaussian for optimized structures in vacuum using static frequencies (i.e., zero-frequency, static electric fields) as a derivative of dipole moment at the DFT level using the Restricted PBE exchange correlation functional and 6-31G++(3df,3pd) basis set.

AUTHOR INFORMATION

Corresponding Author

*(V.I.V.) Bourns Hall A-220, University of California, Riverside, CA 92521. Telephone (951) 827-6239. Fax: (951) 827-6416. E-mail: vullev@ucr.edu. (R.K.L.) 437 Engineering II, University of California, Riverside, CA 92521. Telephone: (951) 827-2122. Fax: (951) 827-2425. E-mail: rlake@ee.ucr.edu. (C.S.O.) Bourns Hall A-305, University of California, Riverside, CA 92521. Telephone: (951) 827-5016. Fax: (951) 827-2899. E-mail: cozkan@engr.ucr.edu. (M.O.) 436 Engineering II, University of California, Riverside, CA 92521. Telephone: (951) 827-2900. Fax: (951) 827-5696. E-mail: mihri@ee.ucr.edu.

Present Addresses

#Department of Biomedical Engineering, Johns Hopkins University, Baltimore, MD 21205.

∇Department of Electrical and Computer Engineering, University of California, Berkeley, CA 94720.

◆Department of Chemistry, University of California, Los Angeles, CA 90095.

ACKNOWLEDGMENT

This research was supported by the National Science Foundation (CBET 0935995, DBI 0731660, EEC 0649096, CMMI 0800680, DMR 0213695, and CMMI 0531171), and by the DARPA/SRC Center on Functional Engineered and Nano Architectonics (FENA).

REFERENCES

(1) Launey, M. E.; Buehler, M. J.; Ritchie, R. O. On the mechanistic origins of toughness in bone. *Annu. Rev. Mater. Res.* **2010**, *40*, 25–53.

(2) Petrasek, J.; Schwarzerova, K. Actin and microtubule cytoskeleton interactions. *Current Opinion in Plant Biology* **2009**, *12*, 728–734.

(3) Hackney, D. D. Processive Motor Movement. *Science* **2007**, *316*, 58–59.

(4) Sowa, Y.; Berry, R. M. The bacterial flagellar motor. *Single Molecule Biology* **2009**, 105–142.

(5) van den Heuvel, M. G. L.; Dekker, C. Motor Proteins at Work for Nanotechnology. *Science* **2007**, *317*, 333–336.

(6) Trinkle-Mulcahy, L.; Lamond Angus, I. Toward a high-resolution view of nuclear dynamics. *Science* **2007**, *318*, 1402–1407.

(7) Alber, F.; Dokudovskaya, S.; Veenhoff, L. M.; Zhang, W.; Kipper, J.; Devos, D.; Suprapto, A.; Karni-Schmidt, O.; Williams, R.; Chait, B. T.; Sali, A.; Rout, M. P. The molecular architecture of the nuclear pore complex. *Nature* **2007**, *450*, 695–701.

(8) Dolezal, P.; Likic, V.; Tachezy, J.; Lithgow, T. Evolution of the molecular machines for protein import into mitochondria. *Science* **2006**, *313*, 314–318.

(9) Hardie, R. C. Dynamic platforms. *Nature* **2007**, *450*, 37–39.

(10) Slessareva, J. E.; Dohlman, H. G. G Protein Signaling in Yeast: New Components, New Connections, New Compartments. *Science* **2006**, *314*, 1412–1413.

(11) Knoblich, J. A. Sara Splits the Signal. *Science* **2006**, *314*, 1094–1096.

(12) Rexach, J. E.; Clark, P. M.; Hsieh-Wilson, L. C. Chemical approaches to understanding O-GlcNAc glycosylation in the brain. *Nature Chem. Biol.* **2008**, *4*, 97–106.

(13) Barglow, K. T.; Cravatt, B. F. Activity-based protein profiling for the functional annotation of enzymes. *Nature Methods* **2007**, *4*, 822–827.

(14) Petricoin, E. F.; Belluco, C.; Araujo, R. P.; Liotta, L. A. The blood peptidome: a higher dimension of information content for cancer biomarker discovery. *Nature Rev. Cancer* **2006**, *6*, 961–967.

(15) Weerapana, E.; Simon, G. M.; Cravatt, B. F. Disparate proteome reactivity profiles of carbon electrophiles. *Nature Chem. Biol.* **2008**, *4*, 405–407.

(16) Suydam, I. T.; Snow, C. D.; Pande, V. S.; Boxer, S. G. Electric Fields at the Active Site of an Enzyme: Direct Comparison of Experiment with Theory. *Science* **2006**, *313*, 200–204.

(17) Sigala, P. A.; Fafarman, A. T.; Bogard, P. E.; Boxer, S. G.; Herschlag, D. Do Ligand Binding and Solvent Exclusion Alter the Electrostatic Character within the Oxyanion Hole of an Enzymatic Active Site? *J. Am. Chem. Soc.* **2007**, *129*, 12104–12105.

(18) Kundrotas, P. J.; Alexov, E. Electrostatic properties of protein−protein complexes. *Biophys. J.* **2006**, *91*, 1724–1736.

(19) Dudev, T.; Lim, C. Principles Governing Mg, Ca, and Zn Binding and Selectivity in Proteins. *Chem. Rev.* **2003**, *103*, 773–787.

(20) Prasad, C. V.; Sundaram, K. On the polarity of the amide group and its impact on dipeptide conformation. *Int. J. Quantum Chem.* **1979**, *15*, 783–792.

(21) Makarenko, V. E.; Makovetskii, V. P.; Borovikov, Y. Y. Electronic structure of some amides from dipole moment measurements and quantum-chemical calculations. *Ukr. Khim. Zh.* **1991**, *57*, 444–448.

(22) Wada, A. Dielectric properties of polypeptide solutions. II. Relation between the electric dipole moment and the molecular weight of the alpha-helix. *J. Chem. Phys.* **1959**, *30*, 328–329.

(23) Hol, W. G. J. Effects of the alpha-helix dipole upon the functioning and structure of proteins and peptides. *Adv. Biophys.* **1985**, *19*, 133–165.

(24) Shin, Y.-G. K.; Newton, M. D.; Isied, S. S. Distance Dependence of Electron Transfer Across Peptides with Different Secondary Structures: The Role of Peptide Energetics and Electronic Coupling. *J. Am. Chem. Soc.* **2003**, *125*, 3722–3732.

(25) Doig, A. J. Recent advances in helix-coil theory. *Biophys. Chem.* **2002**, *101−102*, 281–293.

(26) Mopsik, F. I.; Broadhurst, M. G. Molecular dipole electrets. *J. Appl. Phys.* **1975**, *46*, 4204–4208.

(27) Qiu, X. Patterned piezo-, pyro-, and ferroelectricity of poled polymer electrets. *J. Appl. Phys.* **2010**, *108*, 011101/011101–011101/011119.

(28) Hol, W. G. J.; Van Duijnen, P. T.; Berendsen, H. J. C. The alpha -helix dipole and the properties of proteins. *Nature* **1978**, *273*, 443–446.

(29) Doyle, D. A.; Cabral, J. M.; Pfuetzner, R. A.; Kuo, A.; Gulbis, J. M.; Cohen, S. L.; Chait, B. T.; MacKinnon, R. The structure of the potassium channel: molecular basis of K^+ conduction and selectivity. *Science* **1998**, *280*, 69–77.

(30) Dutzler, R.; Campbell, E. B.; Cadene, M.; Chait, B. T.; MacKinnon, R. X-ray structure of a ClC chloride channel at 3.0 Å reveals the molecular basis of anion selectivity. *Nature* **2002**, *415*, 287–294.

(31) Galoppini, E.; Fox, M. A. Effect of the Electric Field Generated by the Helix Dipole on Photoinduced Intramolecular Electron Transfer in Dichromophoric α-Helical Peptides. *J. Am. Chem. Soc.* **1996**, *118*, 2299–2300.

(32) Yasutomi, S.; Morita, T.; Imanishi, Y.; Kimura, S. A Molecular Photodiode System That Can Switch Photocurrent Direction. *Science (Washington, DC)* **2004**, *304*, 1944–1947.

(33) Ashraf, M. K.; Pandey, R. R.; Lake, R. K.; Millare, B.; Gerasimenko, A. A.; Bao, D.; Vullev, V. I. Theoretical design of bioinspired macromolecular electrets based on anthranilamide derivatives. *Biotechnol. Prog.* **2009**, *25*, 915–922.

(34) Vullev, V. I. From Biomimesis to Bioinspiration: What's the Benefit for Solar Energy Conversion Applications? *J. Phys. Chem. Lett.* **2011**, *2*, 503–508.

(35) Jones, G., II; Vullev, V. I. Photoinduced Electron Transfer between Non-Native Donor-Acceptor Moieties Incorporated in Synthetic Polypeptide Aggregates. *Org. Lett.* **2002**, *4*, 4001–4004.

(36) Jones, G., II; Vullev, V.; Braswell, E. H.; Zhu, D. Multistep Photoinduced Electron Transfer in a de Novo Helix Bundle: Multimer Self-Assembly of Peptide Chains Including a Chromophore Special Pair. *J. Am. Chem. Soc.* **2000**, *122*, 388–389.

(37) Wan, J.; Ferreira, A.; Xia, W.; Chow, C. H.; Takechi, K.; Kamat, P. V.; Jones, G.; Vullev, V. I. Solvent dependence of the charge-transfer properties of a quaterthiophene-anthraquinone dyad. *J. Photochem. Photobiol., A: Chem.* **2008**, *197*, 364–374.

(38) Jones, G., II; Zhou, X.; Vullev, V. I. Photoinduced electron transfer in alpha -helical polypeptides: dependence on conformation and electron donor-acceptor distance. *Photochem. Photobiol. Sci.* **2003**, *2*, 1080–1087.

(39) Jones, G., II; Lu, L. N.; Vullev, V.; Gosztola, D.; Greenfield, S.; Wasielewski, M. Photoactive peptides. 6. Photoinduced electron transfer for pyrenesulfonamide conjugates of tryptophan-containing peptides. Mitigation of fluoroprobe behavior in N-terminal labeling experiments. *Bioorg. Med. Chem. Lett.* **1995**, *5*, 2385–2390.

(40) Vullev, V. I.; Jones, G., II Photoinduced charge transfer in helical polypeptides. *Res. Chem. Intermed.* **2002**, *28*, 795–815.

(41) Vullev, V. I.; Jones, G. Photoinduced electron transfer in alkanoylpyrene aggregates in conjugated polypeptides. *Tetrahedron Lett.* **2002**, *43*, 8611–8615.

(42) Debye, P. J. W. *Polar Molecules*; Dover Publications, Inc.: New York, 1945.

(43) Hurdis, E. C.; Smyth, C. P. Dipole moments in the vapor state and resonance effects in some substituted benzenes. *J. Am. Chem. Soc.* **1942**, *64*, 2212–2216.

(44) Nace, H. R.; Nealey, R. H. Dipole moment and conformation of substituted cyclohexanols. *J. Am. Chem. Soc.* **1966**, *88*, 65–68.

(45) Steimle, T. C.; Nachman, D. F.; Fletcher, D. A. Laboratory measurement of the permanent electric dipole moment of gas-phase copper oxide (CuO) in its X2Pi state. *J. Chem. Phys.* **1987**, *87*, 5670–5673.

(46) Canagaratna, M.; Ott, M. E.; Leopold, K. R. Determination of the dipole moment of $H_3N{-}SO_3$ in the gas phase. *Chem. Phys. Lett.* **1997**, *281*, 63–68.

(47) Jraij, A.; Allouche, A. R.; Rabilloud, F.; Korek, M.; Aubert-Frecon, M.; Rayane, D.; Compagnon, I.; Antoine, R.; Broyer, M.; Dugourd, P. Electric dipole, polarizability and structure of cesium chloride clusters with one-excess electron. *Chem. Phys.* **2006**, *322*, 298–302.

(48) Breitung, E. M.; Vaughan, W. E.; McMahon, R. J. Measurement of solute dipole moments in dilute solution: A simple three-terminal cell. *Rev. Sci. Instrum.* **2000**, *71*, 224–227.

(49) Tjahjono, M.; Davis, T.; Garland, M. Three-terminal capacitance cell for stopped-flow measurements of very dilute solutions. *Rev. Sci. Instrum.* **2007**, *78*, 023902/023901–023902/023906.

(50) Hedestrand, G. Die Berechnung der Molekularpolarisation gelöster Stoffe bei unendlicher Verdünnung. *Z. Phys. Chem.* **1929**, *2*, 428–444.

(51) Halverstadt, I. F.; Kumler, W. D. Solvent polarization error and its elimination in calculating dipole moments. *J. Am. Chem. Soc.* **1942**, *64*, 2988–2992.

(52) Taylor, W. J. Apparent and Partial Molar Polarizations in Solutions and Halverstadt-Kumler and Hedestrand Equations. *J. Phys. Chem.* **1975**, *79*, 1817–1820.

(53) Leontyev, I.; Stuchebrukhov, A. Accounting for electronic polarization in non-polarizable force fields. *Phys. Chem. Chem. Phys.* **2011**, *13*, 2613–2626.

(54) Bao, D.; Millare, B.; Xia, W.; Steyer, B. G.; Gerasimenko, A. A.; Ferreira, A.; Contreras, A.; Vullev, V. I. Electrochemical Oxidation of Ferrocene: A Strong Dependence on the Concentration of the Supporting Electrolyte for Nonpolar Solvents. *J. Phys. Chem. A* **2009**, *113*, 1259–1267.

(55) Onsager, L. Electric moments of molecules in liquids. *J. Am. Chem. Soc.* **1936**, *58*, 1486–1493.

(56) Myers, A. B.; Birge, R. R. The Experimental-Determination of Ground-State Dipole-Moments from Dielectric-Constant Measurements Using Ellipsoidal Cavity Correction Factors. *J. Chem. Phys.* **1981**, *74*, 3514–3521.

(57) Vlassiouk, I.; Smirnov, S. Electric polarization of dilute polar solutions: Revised treatment for arbitrary shaped molecules. *J Phys Chem A* **2003**, *107*, 7561–7566.

(58) Kirkwood, J. G. The dielectric polarization of polar liquids. *J. Chem. Phys.* **1939**, *7*, 911–919.

(59) Malecki, J.; Nowak, J.; Balanicka, S. Extrapolation Method for the Determination of Electric-Dipole Moments from Solutions in Polar-Solvents. *J. Phys. Chem.* **1984**, *88*, 4148–4152.

(60) Böttcher, C. J. F. *Theory of Electric Polarization*, 2nd ed.; Elsevier Scientific Publishing Company: Dordrecht, The Netherlands, 1973; Vol. I, Dielectrics Static Fields.

(61) Frisch, M. J.; Trucks, G. W.; Schlegel, H. B.; Scuseria, G. E.; Robb, M. A.; Cheeseman, J. R.; Montgomery, J. A., Jr.; Vreven, T.; Kudin, K. N.; Burant, J. C.; Millam, J. M.; Iyengar, S. S.; Tomasi, J.; Barone, V.; Mennucci, B.; Cossi, M.; Scalmani, G.; Rega, N.; Petersson, G. A.; Nakatsuji, H.; Hada, M.; Ehara, M.; Toyota, K.; Fukuda, R.; Hasegawa, J.; Ishida, M.; Nakajima, T.; Honda, Y.; Kitao, O.; Nakai, H.; Kiene, M.; Li, X.; Knox, J. E.; Hratchian, H. P.; Cross, J. B.; Bakken, V.; Adamo, C.; Jaramillo, J.; Gomperts, R.; Stratmann, R. E.; Yazyev, O.; Austin, A. J.; Cammi, R.; Pomelli, C.; Ochterski, J. W.; Ayala, P. Y.; Morokuma, K.; Voth, G. A.; Salvador, P.; Dannenberg, J. J.; Zakrzewski, V. G.; Dapprich, S.; Daniels, A. D.; Strain, M. C.; Farkas, O.; Malick, D. K.; Rabuck, A. D.; Raghavachari, K.; Foresman, J. B.; Ortiz, J. V.; Cui, Q.; Baboul, A. G.; Clifford, S.; Cioslowski, J.; Stefanov, B. B.; Liu, G.; Liashenko, A.; Piskorz, P.; Komaromi, I.; Martin, R. L.; Fox, D. J.; Keith, T.; Al-Laham, M. A.; Peng, C. Y.; Nanayakkara, A.; Challacombe, M.; Gill, P. M. W.; Johnson, B.; Chen, W.; Wong, M. W.; Gonzalez, C.; Pople, J. A. *Gaussian 03, Revision C.02*; Gaussian, Inc.: Wallingford, CT, 2004.

(62) Bao, D.; Ramu, S.; Contreras, A.; Upadhyayula, S.; Vasquez, J. M.; Beran, G.; Vullev, V. I. Electrochemical Reduction of Quinones: Interfacing Experiment and Theory for Defining Effective Radii of Redox Moieties. *J. Phys. Chem. B* **2010**, *114*, 14467–14479.

(63) Kurland, R. J.; Wilson, E. B. Microwave Spectrum, Structure, Dipole Moment, and Quadrupole Couplin Constants of Formamide. *J. Chem. Phys.* **1957**, *27*, 585–590.

(64) Bates, W. W.; Hobbs, M. E. The Dipole Moments of Some Acid Amides and the Structure of the Amide Group. *J. Am. Chem. Soc.* **1951**, *73*, 2151–2156.

(65) Sit, S. K.; Dutta, K.; Acharyya, S.; Majumder, T. P.; Roy, S. Double relaxation times, dipole moments, energy parameters and molecular structures of some aprotic polar molecules from relaxation phenomena. *J. Mol. Liq.* **2000**, *89*, 111–126.

(66) Foresman, J. B.; Keith, T. A.; Wiberg, K. B.; Snoonian, J.; Frisch, M. J. Solvent effects 0.5. Influence of cavity shape, truncation of electrostatics, and electron correlation ab initio reaction field calculations. *J. Phys. Chem.* **1996**, *100*, 16098–16104.

(67) Miertus, S.; Scrocco, E.; Tomasi, J. Electrostatic Interaction of a Solute with a Continuum - a Direct Utilization of Abinitio Molecular Potentials for the Prevision of Solvent Effects. *Chem. Phys.* **1981**, *55*, 117–129.

(68) Hu, J.; Xia, B.; Bao, D.; Ferreira, A.; Wan, J.; Jones, G.; Vullev, V. I. Long-Lived Photogenerated States of α-Oligothiophene-Acridinium Dyads Have Triplet Character. *J. Phys. Chem. A* **2009**, *113* 3096–3107.

(69) Voth, A. R.; Khuu, P.; Oishi, K.; Ho, P. S. Halogen bonds as orthogonal molecular interactions to hydrogen bonds. *Nat. Chem.* **2009**, *1*, 74–79.

(70) Hunter, E. C. E.; Partington, J. R. Studies in dielectric polarisation Part V Benzene solutions of pyrones, thiopyrones, and thioketones dtoxan soluttons of ureas and thioureas. *J. Chem. Soc.* **1933**, 87–90.

(71) Smyth, C. P.; Walls, W. S. Electric moment and molecular structure. IV. The glycols. *J. Am. Chem. Soc.* **1931**, *53*, 2115–2122.

(72) Williams, J. W. The dielectric constants of binary mixtures. X. The electric moments of simple derivatives of cyclohexane and of dioxan. *J. Am. Chem. Soc.* **1930**, *52*, 1831–1837.

(73) Aminabhavi, T. M.; Gopalakrishna, B. Density, Viscosity, Refractive-Index, and Speed of Sound in Aqueous Mixtures of *N*,*N*-Dimethylformamide, Dimethyl-Sulfoxide, *N*,*N*-Dimethylacetamide, Acetonitrile, Ethylene-Glycol, Diethylene Glycol, 1,4-Dioxane, Tetrahydrofuran, 2-Methoxyethanol, and 2-Ethoxyethanol at 298.15 K. *J. Chem. Eng. Data* **1995**, *40*, 856–861.

(74) Dotremont, C.; Goethaert, S.; Vandecasteele, C. Pervaporation behaviour of chlorinated hydrocarbons through organophilic membranes. *Desalination* **1993**, *91*, 177–186.

(75) Reinhart, P. B.; Williams, Q.; Weatherly, T. L. Microwave Measurements of Dipole Moments of $CFCl_3$ and $CHCl_3$ and Their Pressure-Broadened Spectra. *J. Chem. Phys.* **1970**, *53*, 1418–.

(76) Sato, K.; Ohkubo, Y.; Moritsu, T.; Ikawa, S.; Kimura, M. Far-Infrared Absorption Intensities and Dipole-Moments of Some Molecules in Solutions. *J. Chem. Soc. Jpn.* **1978**, *51*, 2493–2495.

(77) Antony, A. A.; Smyth, C. P. Microwave Absorption and Molecular Structure in Liquids .LIII. Hydrogen Bonding and Dielectric Properties in Chloroform Mixtures. *J. Am. Chem. Soc.* **1964**, *86*, 152–156.

(78) Thomas, J. R.; Gwinn, W. D. The Rotational Configuration and Dipole Moments of 1,1,2-Trichloroethane and 1,1,2,2-Tetrachloroethane. *J. Am. Chem. Soc.* **1949**, *71*, 2785–2790.

(79) Kiyohara, O.; Higasi, K. I. Dipole Moments of 1,2-Dihalogeno- and 1,1,2,2-Tetrahalogenoethanes in Aromatic and Non-Aromatic Solvents. *Bull. Chem. Soc. Jap.* **1969**, *42*, 1158–1159.

(80) Makosz, J. J. Dipole moment of molecules determined from dielectric measurements in very dilute solutions of a dipole liquid in a nondipole liquid. *J. Mol. Liq.* **1994**, *59*, 103–113.

(81) Lumbroso, H.; Cure, J.; Konakahara, T.; Sato, K. The Polarity of the Oxy Sulfur Bond in Dimethylsulfoxide and Sulfone, Alkylphenyl and Alkyl-2-Pyrazinyl Sulfones. *J. Mol. Struct.* **1983**, *98*, 277–295.

(82) Pekary, A. E. Dipole moment and far-infrared studies on the dimethyl sulfoxide-iodine complex. *J. Phys. Chem.* **1974**, *78*, 1744–1746.

(83) Jones, G., II; Vullev, V. I. Ground- and Excited-State Aggregation Properties of a Pyrene Derivative in Aqueous Media. *J. Phys. Chem. A* **2001**, *105*, 6402–6406.

(84) Jones, G., II; Vullev, V. I. Contribution of a Pyrene Fluorescence Probe to the Aggregation Propensity of Polypeptides. *Org. Lett.* **2001**, *3*, 2457–2460.

(85) Saito, H.; Tanaka, Y.; Nukada, K. Hydrogen Bond Studies by Nitrogen-14 Nuclear Magnetic Resonance 0.3. Study of Electron Redistribution Associated with Hydrogen Bonding and Metal-Complex Formation of Formamide and N-Methylacetamide. *J. Am. Chem. Soc.* **1971**, *93*, 1077–.

(86) Vaara, J.; Kaski, J.; Jokisaari, J.; Diehl, P. NMR properties of formamide: A first principles and experimental study. *J Phys Chem A* **1997**, *101*, 5069–5081.

(87) Sunners, B.; Piette, L. H.; Schneider, W. G. Proton Magnetic Resonance Measurements of Formamide. *Can. J. Chem.* **1960**, *38*, 681–688.

(88) Piette, L. H.; Ray, J. D.; Ogg, R. A. Analysis of the Proton Nuclear Magnetic Resonance Spectrum of Formaide by the Double Resonance Technique. *J. Mol. Spectrosc.* **1958**, *2*, 66–72.

(89) Hill, N. E.; Vaughan, W. E.; Price, A. H.; Davies, M. *Dielectric Properties and Molecular Behavior (The Van Nostrand Series in Physical Chemistry)*; Van Nostrand Reinhold Company Ltd.: 1969.

(90) Ramsay, D. A. The Vibration Spectrum and Molecular Configuration of 1:4-Dioxane. *Proc. R. Soc. London, Ser. A* **1947**, *190*, 562–574.

(91) Mark, J. E.; Sutton, C. Dipole-Moments and Conformational Energies of Chloroethanes. *J. Am. Chem. Soc.* **1972**, *94*, 1083–1090.

(92) Cave, R. J.; Burke, K.; Castner, E. W., Jr. Theoretical Investigation of the Ground and Excited States of Coumarin 151 and Coumarin 120. *J. Phys. Chem. A* **2002**, *106*, 9294–9305.

(93) Böttcher, C. J. F.; Bordewijk, P. *Theory of Electric Polarization*; Elsevier Scientific Publishing Company: Amsterdam, 1978; Vol. II, Dielectrics in Time-Dependent Fields.

(94) Tomasi, J.; Mennucci, B.; Cammi, R. Quantum Mechanical Continuum Solvation Models. *Chem. Rev.* **2005**, *105*, 2999–3093.

(95) Woods, C. J.; Mulholland, A. J. Multiscale modelling of biological systems. *Chem. Model.* **2008**, *5*, 13–50.

(96) Sato, H. Electronic structure and chemical reaction in solution. *Understanding Chem. React.* **2003**, *24*, 61–99.

(97) Sanabria, H.; Miller, J. H.; Mershin, A.; Luduena, R. F.; Kolomenski, A. A.; Schuessler, H. A.; Nanopoulos, D. V. Impedance spectroscopy of alpha-beta tubulin heterodimer suspensions. *Biophys. J.* **2006**, *90*, 4644–4650.

(98) Hong, C.; Bao, D.; Thomas, M. S.; Clift, J. M.; Vullev, V. I. Print-and-Peel Fabrication of Microelectrodes. *Langmuir* **2008**, *24*, 8439–8442.

(99) Jones, G., II; Vullev, V. I. Medium Effects on the Stability of Terbium(III) Complexes with Pyridine-2,6-dicarboxylate. *J. Phys. Chem. A* **2002**, *106*, 8213–8222.

(100) Jones, G., II; Vullev, V. I. Medium effects on the photophysical properties of terbium(III) complexes with pyridine-2,6-dicarboxylate. *Photochem. Photobiol. Sci.* **2002**, *1*, 925–933.

(101) Millare, B.; Thomas, M.; Ferreira, A.; Xu, H.; Holesinger, M.; Vullev, V. I. Dependence of the quality of adhesion between polydimethyl siloxane and glass surfaces on the conditions of treatment with oxygen plasma. *Langmuir* **2008**, *24*, 13218–13224.

(102) Chau, K.; Millare, B.; Lin, A.; Upadhyayula, S.; Nuñez, V.; Xu, H.; Vullev, V. I. Dependence of the Quality of Adhesion between Poly(dimethylsiloxane) and Glass Surfaces on the Composition of the Oxidizing Plasma. *Microfluid. Nanofluid.* **2011**, *10*, 907–917.

(103) Vasquez, J. M.; Vu, A.; Schultz, J. S.; Vullev, V. I. Fluorescence enhancement of warfarin induced by interaction with beta-cyclodextrin. *Biotechnol. Prog.* **2009**, *25*, 906–914.

(104) Jones, G., II; Yan, D.; Hu, J.; Wan, J.; Xia, B.; Vullev, V. I. Photoinduced Electron Transfer in Arylacridinium Conjugates in a Solid Glass Matrix. *J. Phys. Chem. B* **2007**, *111*, 6921–6929.

(105) Perdew, J. P.; Burke, K.; Ernzerhof, M. Generalized gradient approximation made simple. *Phys. Rev. Lett.* **1996**, *77*, 3865–3868.

(106) Petersson, G. A.; Bennett, A.; Tensfeldt, T. G.; Allaham, M. A.; Shirley, W. A.; Mantzaris, J. A Complete Basis Set Model Chemistry 0.1. The Total Energies of Closed-Shell Atoms and Hydrides of the 1st-Row Elements. *J. Chem. Phys.* **1988**, *89*, 2193–2218.

(107) Petersson, G. A.; Allaham, M. A. A Complete Basis Set Model Chemistry 0.2. Open-Shell Systems and the Total Energies of the 1st-Row Atoms. *J. Chem. Phys.* **1991**, *94*, 6081–6090.